Laitrakun *J Wireless Com Network* (2021) 2021:67
https://doi.org/10.1186/s13638-020-01890-3

EURASIP Journal on Wireless Communications and Networking

RESEARCH Open Access

Collision-aware distributed detection with population-splitting algorithms

Seksan Laitrakun*

*Correspondence: seksan@siit.tu.ac.th
Sirindhorn International Institute of Technology, Thammasat University, Pathum Thani 12120, Thailand

Abstract

We consider the design of distributed detection algorithms for single-hop, single-channel wireless sensor networks in which sensor nodes send their local decisions to a fusion center (FC) by using a random access protocol. There is also limited time to collect local decisions before a final decision must be made. We thus propose and analyze a modified random access protocol in which the FC combines slotted ALOHA with a population-splitting algorithm called population-splitting-based random access (PSRA) and collision-aware distributed detection according to an estimate-then-fuse approach. Under the PSRA, only sensor nodes whose observations fall in a particular range of reliability will send their decisions in a specific frame by using slotted ALOHA. At the end of the collection time, the FC applies the collision-aware distributed detection to make a final decision. Here, the FC will first observe the state of each time slot—idle, successful, collision—in each frame, use this information to estimate the number of sensor nodes participating in each frame, and, then, compute a final decision using a population-based fusion rule. An approximation of the optimal transmission probability of the slotted ALOHA is determined to minimize the probability of error. Numerical results show that, unlike slotted-ALOHA-based data networks, the transmission probability maximizing the number of successful time slots does not optimize the performance of the proposed distributed detection. Instead, the proposed distributed detection performs best with a transmission probability that induces many collisions.

Keywords: Distributed detection, Decision fusion, Population-splitting algorithms, Slotted ALOHA, Binary sensor networks

1 Introduction

Distributed detection is an application of wireless sensor networks (WSNs) to decide whether an event of interest is happening in a monitored area [1, 2]. Basically, it consists of a set of sensor nodes and a fusion center (FC). Sensor nodes are deployed over this area to observe the event and make local decisions. The sensor nodes send these decisions to the FC over wireless channels. The FC collects the local decisions and applies a fusion rule to compute a final decision about the existence of the event. As a result, designing a distributed detection system will concern about the operations at sensor nodes and the operations at the FC. A basic structure of distributed detection is shown in Fig. 1. Unlike classical detection [3], distributed detection does not involve only detection methods but also communication techniques [4–6], communication protocols

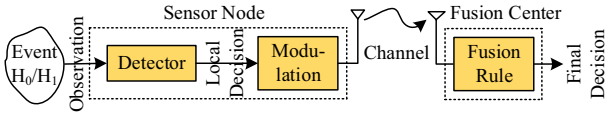

Fig. 1 A basic structure of distributed detection. Distributed detection generally consists of the following basic components: event model, sensor-node processing, channel model, and fusion-center processing

[7–9], transceiver-receiver structures [10–13], transmission channels [14–16], network structures [17–19] etc. An ultimate goal of distributed detection is to derive an optimal fusion rule that is aware of this information. The design of fusion rules is known as a *cross-layer design* problem [20, 21].

Designing distributed detection also encounters a resource-constrained problem. In a large sensor network, the FC might not be able to collect local decisions from all sensor nodes because of limited bandwidth or/and limited time (delay). Therefore, *transmission strategies* between the FC and sensor nodes play an important role to achieve a desired performance under this resource constraint. When the time/banwidth does not allow the FC to collect local decisions from all sensor nodes, the FC might collect only reliable local decisions. This strategy is known as *sensor censoring* [15, 22, 23]. To minimize the collection time or to optimize the performance (given a limited time), distributed detection can be designed such that local decisions are sent to the FC in descending order of their reliability known as *ordered transmissions* [8, 24–26] and *reliability-based splitting algorithms* [9].

A suitable *medium access control (MAC) protocol* is a key to make the transmission strategies above possible in limited bandwidth and time constraints. A problem of applying these transmission strategies is that the transmission scheduling cannot be performed in advance since decision reliability is not known yet. A random access protocol is a method applicable in this scenario. Distributed detection using slotted ALOHA has been studied in many papers [7–9, 20], where sensor nodes randomly choose time slots to send their decisions. However, if two or more decisions are sent at the same time slot, a collision time slot happens. The distributed detection schemes in these papers neglect the collision time slots since the local decisions on these time slots cannot be recovered. Therefore, their performance drops as the number of collisions increases.

1.1 Contributions

In this paper, we study a distributed detection system with a large number of sensor nodes N. A time duration T time slots (assume $T \ll N$) over a single channel is provided to collect local decisions. If two or more sensor nodes send their local decisions at the same time slot, a packet collision happens and the FC cannot decode the transmitted local decisions inside this time slot. Since T is less than N, the FC can collect only some local decisions but not all of them. For example, in a distributed detection system using the time division multiple access (TDMA) as its MAC protocol, the FC will be able to collect only up to T local decisions. Therefore, the collection time T will limit the performance of this distributed detection.

We are interested in jointly designing a transmission strategy, a MAC protocol, and fusion rules at the FC to improve the performance of the distributed detection with a limited collection time over a single channel. A key design is that, with properly revising a transmission strategy and a random access protocol such that the packet collisions will be from the *same* local decisions, a packet collision indicates two or more sensor nodes have the same decision. As a result, the packet collisions are informative [27–30]. The main contributions and results of this paper can be summarized as follows.

We propose a transmission protocol (i.e., a transmission strategy and a MAC protocol) based on a population-splitting algorithm called *population-splitting-based random access* (PSRA), which is a modification of slotted ALOHA. We use the term "population splitting" because the sensor nodes (i.e., population) are split into groups based on their observation values. By using this algorithm, the observation range is divided into censored regions (unreliable observations) and M uncensored regions (reliable observations). Only groups of sensor nodes whose observations are in the uncensored regions will send their data to the FC. We also divide the collection time T into M frames, where each frame contains K time slots. The sensor nodes whose observations are in the mth uncensored region will send their data in the mth frame. Since the frame itself indicates the observation region (i.e., the local data found in the mth frame corresponds to the observation in the mth uncensored region), we assume that the sensor nodes send a data bit 1 (i.e., no need to make a local decision). However, because we do not know which sensor nodes will send their data bits in the mth frame, a fixed transmission scheduling such as TDMA cannot be applied. A slotted ALOHA protocol is exploited. A sensor node whose observation is in the mth region will send the data bit at a time slot in the mth frame with a probability $\frac{\rho_m}{K}$, where ρ_m is called *transmission probability* at the mth frame. The parameter ρ_m indicates the probability that a sensor node whose observation is in the mth region will send its data in the mth frame. The scaling $\frac{1}{K}$ is a normalized factor (per frame). By using a slotted ALOHA protocol, collision time slots, when two or more sensor nodes send their data bits at the same time slot, will happen. However, unlike [7–9, 20], we design and propose *collision-aware* distributed detection whose FC is aware of collisions and utilizes them in making a final decision.

The performance of the collision-aware distributed detection is affected by the transmission probabilities $\boldsymbol{\rho} = (\rho_1, \rho_2, \ldots, \rho_M)$, where ρ_m controls the number of sensor nodes sending the data bits in the mth frame (i.e., network traffic). A higher value of ρ_m induces a larger number of collision time slots in that frame. We, then, propose a method to approximate the optimal transmission probabilities, which minimize the probability of error. We can show that, for the collision-aware distributed detection scheme, unlike data networks [31], the transmission probabilities maximizing the throughput are not optimal. On the other hand, the numerical results show that the transmission probabilities inducing a lot of collision time slots are optimal. This is because, in the collision-aware distributed detection, the collision time slots are informative.

1.2 Related work

Transmission strategies have been broadly exploited to improve the performance of distributed detection in a resource-constrained scenario. In addition to sensor censoring [15, 22, 23, 32], ordered transmissions [8, 24–26], and reliability-based

splitting algorithms [9], a transmission strategy called *type-based multiple access* (TBMA) has been proposed [33, 34] over a multiple access channel. In the TBMA scheme, the observation is quantized into M levels and M orthogonal waveforms $\{\phi_m(t)\}$, for $m = 1, 2, \ldots, M$, are provided. Sensor nodes whose observations are in the mth level will send a waveform $\phi_m(t)$ to the FC. The received waveforms are then combined to each other. The amplitude of the waveform $\phi_m(t)$ detected at the FC indicates the number of sensor nodes in the mth level, which will be used further in making a final decision. As an extension of the TBMA, a transmission strategy called *type-based random access* (TBRA) over a multiple access channel has been proposed in [35]. The term "random" here emphasizes that the number of sensor nodes involving in transmissions is random. Our proposed PSRA is different from the TBMA and TBRA in the following aspects. First, we study a problem of distributed detection when only a single collision channel is provided. Second, in the PSRA, the sensor nodes whose observations are in the mth level will send their data bits in the mth frame using slotted ALOHA. As a result, the FC observes the states of time slots (i.e., idle, successful, collision time slots) in making a final decision.

Random-access protocols have been applied in many distributed detection schemes especially when a proper transmission scheduling is not allowed [7–9, 20]. However, packet collisions, as an intrinsic property of random access, deteriorate the performance of the schemes in these papers since the packet collisions are neglected. With properly revising a transmission strategy such that the packet collisions will be from the same data, a packet collision indicates two or more sensor nodes have the same data. As a result, the packet collisions can be used in making a final decision [27–30]. Similarly, in the proposed PSRA, since the data bits sent in the same frame will be from the observations in the same level, the collision time slots in each frame are meaningful and will be used in making a final decision.

Transmission protocols based on population-splitting algorithms for distributed detection/estimation have been studied in [29, 36, 37], where the sensor nodes will share a collision channel to send their decisions. By using these protocols, the observation range is divided into M levels and the collect time is divided into M frames. The sensor nodes whose observations are in the mth level will send their decisions in the mth frame. The FC observes the time-slot states to make a final decision or compute an estimate. The transmission protocol proposed in this paper is different from those in [29, 36, 37] as follows. Here, we apply the sensor-censoring strategy to a population-splitting algorithm, where the observation range is divided into censored regions (unreliable observations) and uncensored regions (reliable observations). The uncensored regions are further divided into M levels. Only the sensor nodes whose observations are in the uncensored regions will send their data bits in the corresponding frames.

1.3 Organization

The remainder of this paper is organized as follows. The system model is introduced in Sect. 2. Collision-aware distributed detection with a population-splitting algorithm is proposed in Sect. 3. Approximations of the optimal transmission

probabilities are determined in Sect. 4. The numerical results are evaluated and discussed in Sect. 5. Finally, conclusions are provided in Sect. 6.

2 System model

2.1 Centralized fusion system

We consider a distributed detection system with N sensor nodes deployed in an area to monitor an event of interest. To start the local-decision collection process, the FC will broadcast an inquiry about the existence of this event. Each sensor node will draw an observation, compute a data bit, and send it to the FC via a single-hop and shared collision channel by using the transmission protocol proposed in Sect. 3.2.

2.2 Transmission channel

The sensor nodes will share a collision channel to send their data bits to the FC. This collision channel is divided into time slots, with the FC and sensor nodes knowing when a time slot begins and ends (i.e., synchronous time slot). In a collision-channel model, a time slot is classified into the following *time-slot* states [31]:

- a time slot is called as an *idle* time slot if no data packets are sent at this time slot,
- a time slot is called as a *successful* time slot if only one data packet is sent at this time slot,
- a time slot is called as a *collision* time slot if two or more data packets are sent at this time slot.

We assume that the collisions are solely from the transmissions of the sensor nodes in the considered network. The length of each time slot is equal to the packet containing a data bit.

2.3 Binary hypothesis testing model

The noisy observation x at a sensor node is governed by the following binary hypothesis model:

$$H_0 : \ x \sim f_X(x|H_0) \quad \text{and} \quad H_1 : \ x \sim f_X(x|H_1), \tag{1}$$

where $f_X(x|H_i)$ is the conditional probability density function (PDF) of x. The observations are assumed to be *independent and identically distributed* (IID) given H_i, for $i = 0, 1$, and among the sensor nodes and time slots. The prior probability that H_0 happens, $\Pr(H_0)$, is equal to P_0, and, the prior probability that H_1 happens, $\Pr(H_1)$, is equal to $P_1 = 1 - P_0$.

3 Methods

3.1 Overview of the proposed method

We consider a distributed detection system with a shared collision channel and a limited collection time. There are N sensor nodes deployed in the area to monitor whether the event H_0 or the event H_1 happens. These sensor nodes will send their decisions over a shared collision channel to the FC. The FC is allowed to collect local

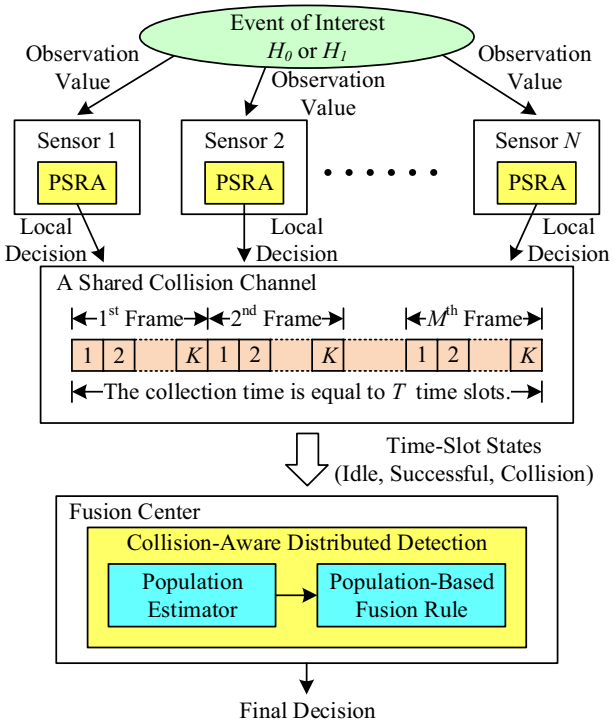

Fig. 2 A diagram to display the proposed method. There are N sensor nodes in the area to monitor the status of the event of interest. These sensor nodes send their decisions to the FC over a shared collision channel by using the PSRA protocol. At the end of the collection time T time slots, the FC observes the time-slot states and make a final decision by using the collision-aware distributed detection

decisions within a time duration equal to T time slots, which is less than the number of nodes N. As a result, the FC cannot collect all local decisions from N sensor nodes. To handle this issue and improve the performance of this distributed detection system, we propose *collision-aware distributed detection with a population-splitting algorithm*.

The proposed method consists of two parts: a transmission protocol called *population-splitting-based random access* (PSRA) and a detection strategy called *collision-aware distributed detection*. As shown in Fig. 2, each sensor node will apply the PSRA to send its decision over a shared channel to the FC. By using the PSRA, the collection time (whose length is equal to T time slots) is organized into M frames (each frame consists of K time slots) and the observation range is divided into censored regions and M uncensored regions. The sensor nodes whose observations are within a *censored region* will decide not to send their decisions to the FC. On the other hand, the sensor nodes whose observations are within the mth *uncensored region* will send their binary bits $b = 1$ at a time slot in the m*th* frame by using a slotted Aloha protocol. At the end of the collection time T, the FC will observe the time-slot states (idle, successful, and collision) in each frame and use them to estimate the number of sensor nodes ($\hat{n}_m$, for $1 \leq m \leq M$) who send their binary bits in that frame by using the

population estimator. Finally, the FC applies these estimated node numbers $\hat{n}_1$, $\hat{n}_2$, ..., $\hat{n}_M$ into the *population-based fusion rule* to make a final decision whether the event H_0 or the event H_1 happens. The details of the transmission protocol PSRA and the collision-aware distributed detection are explained in Sects. 3.2 and 3.3, respectively.

3.2 Population-splitting-based random access

The PSRA is shown in Algorithm 1. The censored regions and uncensored regions are chosen according to the observation reliability [9]. The censored regions cover the ranges of those unreliable observations, which are unlikely to help in detection. On the other hand, the uncensored regions consist of the ranges of reliable observation, which would be useful in detection. Only the sensor nodes whose observations are in the uncensored regions might send their data bits $b = 1$ to the FC.

Algorithm 1 Population-Splitting-Based Random Access

The range of the observation x is divided into I censored regions $(\mathcal{C}_1, \mathcal{C}_2, \ldots, \mathcal{C}_I)$ and M uncensored regions $(\mathcal{U}_1, \mathcal{U}_2, \ldots, \mathcal{U}_M)$, where

$$\mathcal{C}_i = \{x : \nu_i^L < x \leq \nu_i^U\}, \quad \mathcal{U}_m = \{x : \tau_m^L < x \leq \tau_m^U\}, \tag{2}$$

while ν_i^L, ν_i^U, τ_m^L, and τ_m^U are thresholds. In addition, the collection time T is divided into M frames, where each frame consists of K time slots, as shown in Fig. 3. By using the population-splitting-based random access, the sensor nodes perform the following steps:

1. At the beginning of the collection time, each sensor node draws a new observation x.
2. The sensor nodes whose $x \in \mathcal{U}_m$ (i.e., the observation is in an uncensored region) will decide to send the data bit $b = 1$ in the mth frame with the transmission probability ρ_m; otherwise, the sensor nodes keep silent.
   - Here, slotted ALOHA is applied. At the beginning of each time slot in this frame, the sensor nodes who decide to send their data bit will send their data bit $b = 1$ at this time slot with a probability $\frac{1}{K}$.
3. The Step 2 above is repeated from $m = 1$ till $m = M$.

The algorithm's specific details are explained and modeled as follows. Let n_m, for $1 \leq m \leq M$, be the number of sensor nodes whose observation $x \in \mathcal{U}_m$. Since the sensor nodes draw an observation at the beginning of the collection time, the variables $n_1, n_2, \ldots, n_M$ can be modeled as multinomial random variables. The probability mass function (PMF) of $\mathbf{n} = (n_1, n_2, \ldots, n_M)$ given H_i is expressed as

$$\Pr(\mathbf{n}|H_i) = \frac{N!}{n_1! n_2! \cdots n_{M+1}!} q_{1|i}^{n_1} q_{2|i}^{n_2} \cdots q_{M+1|i}^{n_{M+1}}, \tag{3}$$

where $0 \leq n_m \leq N$, $q_{m|i} = \int_{\tau_m^L}^{\tau_m^U} f_X(x|H_i)\, dx$, $n_{M+1} = N - \sum_{m=1}^{M} n_m$, and $q_{M+1|i} = 1 - \sum_{m=1}^{M} q_{m|i}$. The set $\mathbf{n} = (n_1, n_2, \ldots, n_M)$ can be used to differentiate whether the event H_0 or H_1 is happening. Note that $q_{m|i}$ is the probability that an observation value will be in the mth uncensored region and $q_{M+1|i}$ is the probability that an observation value will be in the censored regions.

Each frame is used to indicate an uncensored region $\mathcal{U}_m$. The sensor nodes who have their observation $x \in \mathcal{U}_m$ will send their data bits $b = 1$ in the mth frame with a probability ρ_m (the rest will keep silent). However, these sensor nodes are unknown. Transmission scheduling cannot be arranged in advance. We, then, apply slotted

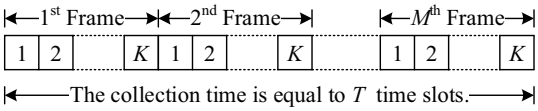

Fig. 3 The structure of the collection time. The collection time (T time slots) is divided into M frames, where each frame consists of K time slots

ALOHA to handle the multiple access problem. In each time slot, these sensor nodes will decide to send their data bit with the probability $\frac{1}{K}$. Similar to [27–29], a collision time slot is meaningful and recognized since a collision time slot indicates that there are two or more sensor nodes whose observation $x \in \mathcal{U}_m$ (Fig. 3).

At the end of each time slot, the FC observes the state of that time slot. Let $d_{k,m}$ be the time-slot state of the kth time slot in the mth frame. We have $d_{k,m} \in \{0, \text{S}, \text{C}\}$, where $d_{k,m} = 0$, $d_{k,m} = \text{S}$, and $d_{k,m} = \text{C}$ indicate the idle time slot, the successful time slot, and the collision time slot, respectively. Therefore, a time slot will be an idle, successful, or collision time slot with the following conditional probabilities:

$$\begin{aligned}
\Pr(d_{k,m} = 0|n_m) &= p_{0,m} = \left(1 - \frac{\rho_m}{K}\right)^{n_m}, \\
\Pr(d_{k,m} = \text{S}|n_m) &= p_{\text{S},m} = n_m \left(\frac{\rho_m}{K}\right)\left(1 - \frac{\rho_m}{K}\right)^{n_m - 1}, \\
\Pr(d_{k,m} = \text{C}|n_m) &= p_{\text{C},m} = 1 - p_{0,m} - p_{\text{S},m}.
\end{aligned} \tag{4}$$

The probabilities $p_{0,m}$, $p_{\text{S},m}$, and $p_{\text{C},m}$ are called as the probability of no transmission, the probability of successful transmission, and the probability of collisions, respectively. As a result, the conditional PMF of $d_{k,m}$ given n_m can be expressed as

$$\Pr(d_{k,m}|n_m) = (p_{0,m})^{\mathbb{1}_{\{d_{k,m}=0\}}} (p_{\text{S},m})^{\mathbb{1}_{\{d_{k,m}=\text{S}\}}} (p_{\text{C},m})^{\mathbb{1}_{\{d_{k,m}=\text{C}\}}}, \tag{5}$$

where $\mathbb{1}_{\{\cdot\}}$ is the indicator function.

At the end of the mth frame, the FC observes the following time-slot states $d_{1,m}, d_{2,m}, \ldots, d_{K,m}$, whose joint conditional PMF is

$$\Pr(\mathbf{d}_m|n_m) = \prod_{k=1}^{K} \Pr(d_{k,m}|n_m), \tag{6}$$

where $\mathbf{d}_m = (d_{1,m}, d_{2,m}, \ldots, d_{K,m})$. In addition, the FC observes that there are $z_{0,m}$ idle time slots (i.e., $d_{k,m} = 0$), $z_{\text{S},m}$ successful time slots (i.e., $d_{k,m} = \text{S}$), and $z_{\text{C},m}$ collision time slots ($d_{k,m} = \text{C}$) in the mth frame. Therefore, the joint PMF (6) is equivalent to, when the FC observes $z_{0,m}$, $z_{\text{S},m}$, and $z_{\text{C},m}$:

$$\Pr(\mathbf{z}_m|n_m) = \frac{K!}{z_{0,m}! z_{\text{S},m}! z_{\text{C},m}!} p_{0,m}^{z_{0,m}} p_{\text{S},m}^{z_{\text{S},m}} p_{\text{C},m}^{z_{\text{C},m}}, \tag{7}$$

where $\mathbf{z}_m = (z_{0,m}, z_{\text{S},m}, z_{\text{C},m})$. Note that $z_{0,m} + z_{\text{S},m} + z_{\text{C},m} = K$. In addition, we can write the joint conditional PMF of $z_{0,m}$, $z_{\text{S},m}$, and $z_{\text{C},m}$ given H_i as

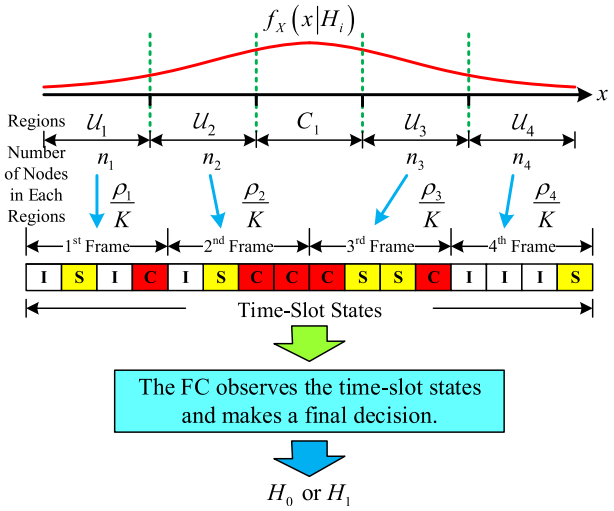

Fig. 4 An example illustrates the idea of the PSRA protocol, where the range of the observation x is divided in to one censored region ($\mathcal{C}_1$) and four uncensored regions ($\mathcal{U}_1, \mathcal{U}_2, \mathcal{U}_3, \mathcal{U}_4$). The collection time ($T$) is equal to 16 and divided into $M = 4$ and $K = 4$. Assume that there are n_m sensor nodes with $x \in \mathcal{U}_m$, for $m = 1, 2, 3, 4$. They will send their data bits at a time slot in the mth frame with a probability $\frac{\rho_m}{K}$. As a result, idle time slots (I), successful time slots (S), and collision time slots (C) will happen

$$\Pr(\mathbf{z}_m|H_i) = \sum_{n_m=0}^{N} \Pr(\mathbf{z}_m|n_m)\Pr(n_m|H_i). \tag{8}$$

At the end of the collection time, the FC has observed the time-slot states $\mathbf{z}_1, \mathbf{z}_2, \ldots, ..\mathbf{z}_M$. The joint conditional PMF of $\mathbf{z} = (\mathbf{z}_1, \mathbf{z}_2, \ldots, ..\mathbf{z}_M)$ given H_i can be expressed as

$$\begin{aligned}\Pr(\mathbf{z}|H_i) &= \prod_{m=1}^{M} \Pr(\mathbf{z}_m|H_i) \\ &= \prod_{m=1}^{M} \sum_{n_m=0}^{N} \Pr(\mathbf{z}_m|n_m)\Pr(n_m|H_i).\end{aligned} \tag{9}$$

Therefore, we devise distributed detection that is *aware* of these collision time slots in addition to successful time slots and idle time slots as shown in Sect. 3.3, where the FC will exploit the time-slot states $\mathbf{z}$ to decide whether H_0 or H_1 is happening.

The transmission probability ρ_m is a key parameter since it controls the network traffic (the number of transmitting nodes) in the mth frame. As a result, numbers of idle, successful, and collision time slots depend on ρ_m. A large value of ρ_m induces a large number of transmitting nodes and a large number of collision time slots in the mth frame. There will be a set of transmission probabilities $\boldsymbol{\rho}^* = (\rho_1^*, \rho_2^*, \ldots, \rho_M^*)$ maximizing the performance of the proposed distributed detection, which will be studied in Sects. 4 and 5. We would like to note that finding the optimal thresholds $\boldsymbol{\nu}^* = (\nu_1^{L*}, \nu_2^{U*}, \ldots, \nu_I^{L*}, \nu_I^{U*})$ and $\boldsymbol{\tau}^* = (\tau_1^{L*}, \tau_1^{U*}, \ldots, \tau_M^{L*}, \tau_M^{U*})$, which is also known as *quantizer design*,[1] is beyond the scope of this paper.

[1] For example, the papers that deals with this problem are [9, 38–42].

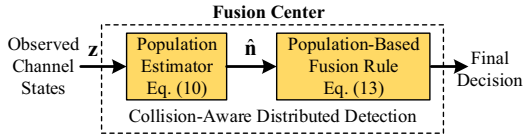

a The proposed collision-aware distributed detection consists of two stages: a population estimator and a population-based fusion rule, where $\mathbf{z}$ is a set of observed time-slot states and $\hat{\mathbf{n}}$ is a set of estimated numbers of sensor nodes in the uncensored regions $\mathcal{U}_1, \mathcal{U}_2, \ldots, \mathcal{U}_M$.

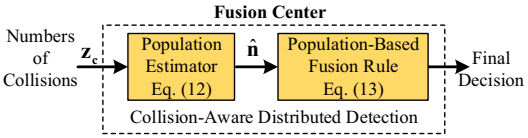

b As shown in Corollary , the FC will need only to observe a set of collision time slots, $\mathbf{z}_{\mathrm{C}} = (z_{\mathrm{C},1}, z_{\mathrm{C},2}, \ldots, z_{\mathrm{C},M})$ to estimate $\hat{\mathbf{n}}$.

Fig. 5 Diagrams to display the structure of the proposed collision-aware distributed detection

An example showing the main idea of the PSRA is provided in Fig. 4. The range of the observation is divided into a censored region ($\mathcal{C}_1$) and four uncensored regions ($\mathcal{U}_1$, $\mathcal{U}_2$, $\mathcal{U}_3$, and $\mathcal{U}_4$). Assume that the event H_i is happening. The distribution of observations is $f_X(x|H_i)$. There is n_m sensor nodes whose observations $x \in \mathcal{U}_m$. According to the PSRA protocol, these sensor nodes will decide to send their data bits at each time slot in the mth frame with the probability $\frac{\rho_m}{K}$. As a result, the FC observes the time-slot state $\mathbf{z}_m = (z_{0,m}, z_{\mathrm{S},m}, z_{\mathrm{C},m})$ in the mth frame, where $z_{0,m}$, $z_{\mathrm{S},m}$, and $z_{\mathrm{C},m}$ are the numbers of the idle, successful, and collision time slots, respectively. The FC will exploit these time-slot states $\mathbf{z}_m$, for $m = 1, 2, \ldots, M$, in making a final decision. Note that if the parallel access channels (PACs)[2] are assumed, the FC would *clearly* see the number of sensor nodes n_m, for $m = 1, 2, \ldots, M$, and would directly use them in making a final decision instead.

3.3 Collision-aware distributed detection: estimate-then-fuse approach

The optimal fusion rule of the proposed distributed detection can be directly derived from $\frac{\Pr(\mathbf{z}|H_1)}{\Pr(\mathbf{z}|H_0)}$, where $\Pr(\mathbf{z}|H_i)$ is from (9). However, this optimal fusion rule is complicated and untraceable in analysis, which no insightful meaning can be discovered or proved. Similar to [1, 4–6, 10–16], we aim to devise suboptimal fusion that allows us to derive some meaningful properties.

In this section, we consider that the FC compute a final decision based on the *estimate-then-fuse* approach [29, 36, 37] as shown in Fig. 5a, which consists of two stages: a population estimator of the node numbers and a population-based fusion rule. First, the FC will use the estimator to compute the estimates of $n_1, n_2, \cdots$, and n_M, which are denoted as $\hat{n}_1, \hat{n}_2, \cdots$, and $\hat{n}_M$, respectively, from the observed time-slot states $\mathbf{z} = (\mathbf{z}_1, \mathbf{z}_2, \ldots, \mathbf{z}_M)$. Thereafter, the FC exploits these estimates $\hat{\mathbf{n}} = (\hat{n}_1, \hat{n}_2, \ldots, \hat{n}_M)$ in the proposed population-based fusion rule. The population estimator and the population-based fusion rule are described next.

[2] An example of PACs is the frequency division multiple access (FDMA). Each sensor node exploits its own frequency channel to send the decision. However, using the PACs is not a bandwidth-efficient approach in this scenario.

In the first stage, the FC will estimate the number of sensor nodes n_m in each frame by exploiting the population estimator. The details are shown in the proposition below. Note that, from now on, we omit the fact that n_m is an integer and, then, consider n_m as a real number instead. Therefore, we can derive and prove some meaningful properties. We would like to note that Proposition 1 and Corollary 1 have been shown in [36, 37].

Proposition 1 (Population estimate) *The maximum-likelihood (ML) estimate of the number of sensor nodes whose $x \in \mathcal{U}_m$ based on the observed time-slot states $\mathbf{z}_m$ is*

$$\hat{n}_m = \underset{n_m \in [0,N]}{\arg\max} \left[z_{0,m} \log(p_{0,m}) + z_{S,m} \log(p_{S,m}) + z_{C,m} \log(p_{C,m}) \right]. \tag{10}$$

For a large K, the PDF of $\hat{n}_m$ can be asymptotically expressed as a Gaussian PDF: $\hat{n}_m \overset{a}{\sim} \mathcal{N}(n_m, \upsilon_m^2)$, where $\overset{a}{\sim}$ denotes "asymptotically distributed according to" and, for a large n_m and $n_m \gg K$,

$$\upsilon_m^2 \approx \left\{ K \left(\frac{1 - p_{C,m}}{p_{C,m}} \right) \left[\log\left(1 - \frac{\rho_m}{K}\right) \right]^2 \right\}^{-1}. \tag{11}$$

Proof An outline of the proof has been shown in [36, 37]. The full derivation is shown in Appendix A. □

Note that the variance υ_m^2 will affect the quality of the proposed distributed detection, which will be discussed in the next section. In addition, we can show that $\log \Pr(\mathbf{z}_m | n_m)$ is a concave function of n_m, and, then, we have an alternative form of the population estimate $\hat{n}_m$ as shown in Corollary 1 below.

Corollary 1 (Equivalent population estimate of n_m) *For a large n_m, the ML estimate $\hat{n}_m$ obtained from (10) is equal to the value n_m satisfying*

$$\frac{1 - p_{C,m}}{p_{C,m}} = \frac{K - z_{C,m}}{z_{C,m}}. \tag{12}$$

Note that n_m is inside $p_{C,m}$.

Proof An outline of the proof has been shown in [36, 37]. The full derivation is shown in Appendix B. □

From Corollary 1, we see that only the number of collision time slots $z_{C,m}$ is needed to estimate n_m. As a result, the input to the diagram of the proposed distributed detection can be revised as shown in Fig. 5b.

In the second stage, the FC will apply the estimates $\hat{\mathbf{n}} = (\hat{n}_1, \hat{n}_2, \ldots, \hat{n}_M)$ into the population-based fusion rule to compute a final decision. The population-based fusion rule is described in the proposition below.

Proposition 2 (Population-based fusion rule given $\hat{\mathbf{n}}$) *Given a set of estimated numbers of sensor nodes,* $\hat{\mathbf{n}} = (\hat{n}_1, \hat{n}_2, \ldots, \hat{n}_M)$. *The population-based fusion rule is expressed as*

$$\Lambda = \sum_{m=1}^{M} \hat{n}_m \left[\log\left(\frac{q_{m|1}}{q_{M+1|1}}\right) - \log\left(\frac{q_{m|0}}{q_{M+1|0}}\right) \right] \underset{H_0}{\overset{H_1}{\gtrless}} \gamma, \tag{13}$$

where the decision threshold γ *is adjusted to achieve the desired performance.*

Proof The test statistic Λ is directly obtained from the following log-likelihood ratio $\Lambda = \frac{\Pr(\mathbf{n}|H_1)}{\Pr(\mathbf{n}|H_0)}\Big|_{\mathbf{n}=\hat{\mathbf{n}}}$, where $\mathbf{n} = (n_1, n_2, \ldots, n_M)$ will be substituted by the estimates $\hat{\mathbf{n}} = (\hat{n}_1, \hat{n}_2, \ldots, \hat{n}_M)$. From (3), we can show that

$$\frac{\Pr(\mathbf{n}|H_1)}{\Pr(\mathbf{n}|H_0)} = N \log\left(\frac{q_{M+1|1}}{q_{M+1|0}}\right) + \sum_{m=1}^{M} n_m \log\left[\left(\frac{q_{m|1}}{q_{M+1|1}}\right) - \log\left(\frac{q_{m|0}}{q_{M+1|0}}\right)\right]. \tag{14}$$

Since the first term on the right-hand side of the equation above is a constant, we can write the test statistic Λ as shown in (13) after replacing $\mathbf{n}$ with $\hat{\mathbf{n}}$. □

Recall that the collision-aware distributed detection here is parameterized by the number of sensor nodes N, the number of frames M, and the number of time slots in a frame K. It is worth to mention the computational complexity of the proposed distributed detection according to these parameters. In the first stage, the FC will estimate the number of sensor nodes $\hat{n}_m$ in each frame according to (10). To do this, the FC will observe and count the numbers of time slot states in each frame (i.e., $z_{0,m}$, $z_{S,m}$, and $z_{C,m}$), compute the probabilities in (4), and, then, check all $n_m \in [0, N]$ by using (10). As a result, for M frames, the first stage incurs the complexity $\mathcal{O}(MK + MN)$. In the second stage, to make a final decision, given the estimate $\hat{n}_m$ from the first stage, the FC applies the fusion rule (13) which requires the complexity $\mathcal{O}(M)$. Finally, the overall computational complexity of the proposed distributed detection is of order $\mathcal{O}(MK + MN + M)$.

4 Approximations of optimal transmission probabilities

The performance of the proposed distributed detection can be shown via the probability of detection (P_D) and the probability of false alarm (P_F). These probabilities are affected by a set of transmission probabilities $\boldsymbol{\rho} = (\rho_1, \rho_2, \ldots, \rho_M)$. A small transmission probability ρ_m will allow only a few sensor nodes to send their data bits in the mth frame, and, then, induce a large number of idle time slots in the mth frame. On the other hand, a large transmission probability ρ_m will allow many sensor nodes to send their data bits in the mth frame, and, then, induce a large number of collision time slots in the mth frame. The transmission probabilities $\boldsymbol{\rho} = (\rho_1, \rho_2, \ldots, \rho_M)$ will impact on the estimation's quality of the ML estimator (shown in Proposition 1), and, then, the final decision's quality of the population-based fusion rule (shown in Proposition 3). Therefore, there will be a set of transmission probabilities $\boldsymbol{\rho}^* = (\rho_1^*, \rho_2^*, \ldots, \rho_M^*)$ optimizing the performance of the proposed distributed detection. However, finding the optimal transmission probabilities $\boldsymbol{\rho}^*$ numerically will be cumbersome. An analytical way is needed. In what follows, we

will derive approximations of the transmission probabilities minimizing the proposed distributed detection's error probability.

We need to derive the conditional PDF of Λ given H_i, denoted by $\Pr(\Lambda|H_i)$. However, the exact form of $\Pr(\Lambda|H_i)$ is not yet found. Instead, we will derive an asymptotic approximation of $\Pr(\Lambda|H_i)$, denoted by $\tilde{\Pr}(\Lambda|H_i)$, as shown in the proposition below.

Proposition 3 (Asymptotic PDF approximation) *An approximation of the conditional PDF of* Λ *given* H_i*, denoted by* $\tilde{\Pr}(\Lambda|H_i)$*, can be expressed as a Gaussian PDF* $\mathcal{N}(\mu_i, \sigma_i^2)$*, for* $i = 0, 1$*, whose*

$$\mu_i = N \sum_{m=1}^{M} q_{m|i} \left[\log\left(\frac{q_{m|1}}{q_{M+1|1}}\right) - \log\left(\frac{q_{m|0}}{q_{M+1|0}}\right) \right], \tag{15}$$

$$\sigma_i^2 = \frac{1}{K} \sum_{m=1}^{M} \frac{\left[\log\left(\frac{q_{m|1}}{q_{M+1|1}}\right) - \log\left(\frac{q_{m|0}}{q_{M+1|0}}\right) \right]^2}{\left(\frac{1-\bar{p}_{\mathrm{C},m|i}}{\bar{p}_{\mathrm{C},m|i}}\right) \left[\log\left(1 - \frac{\rho_m}{K}\right) \right]^2}, \tag{16}$$

where $\bar{n}_{m|i} = Nq_{m|i}$, $\bar{p}_{\mathrm{C},m|i} = 1 - \bar{p}_{0,m|i} - \bar{p}_{\mathrm{S},m|i}$, $\bar{p}_{0,m|i} = (1 - \frac{\rho_m}{K})^{\bar{n}_{m|i}}$, *and* $\bar{p}_{\mathrm{S},m|i} = \bar{n}_{m|i}(\frac{\rho_m}{K})(1 - \frac{\rho_m}{K})^{\bar{n}_{m|i}-1}$.

Proof Please see Appendix C. □

The value $\bar{n}_{m|i}$ is the *average* number of sensor nodes whose $x \in \mathcal{U}_m$ (i.e., in the mth frame) given H_i. Correspondingly, the probabilities $\bar{p}_{0,m|i}$, $\bar{p}_{\mathrm{S},m|i}$, and $\bar{p}_{\mathrm{C},m|i}$ are computed at $\bar{n}_{m|i}$. We see that the variance σ_i^2 from (16) is a weighted sum of the variance υ_m^2 from (11). Therefore, the quality of the estimates $\hat{\boldsymbol{n}}$ from the population estimator will directly affect the quality of the decision making obtained from the population-based fusion rule.

Subsequently, we will approximate a set of transmission probabilities $\boldsymbol{\rho}^\star = (\rho_1^\star, \rho_2^\star, \ldots, \rho_M^\star)$ minimizing the probability of error $P_\mathrm{E} = P_0 P_\mathrm{F} + P_1 P_\mathrm{M}$, where P_M is the probability of miss and equal to $1 - P_\mathrm{D}$. From Proposition 3, we have the following approximations of the probability of detection P_D and the probability of false alarm P_F:

$$P_\mathrm{D} = \tilde{\Pr}(\Lambda > \gamma|H_1) = Q\Big(\frac{\gamma - \mu_1}{\sigma_1}\Big), \tag{17}$$

$$P_\mathrm{F} = \tilde{\Pr}(\Lambda > \gamma|H_0) = Q\Big(\frac{\gamma - \mu_0}{\sigma_0}\Big), \tag{18}$$

where the conditional probability $\tilde{\Pr}(\Lambda|H_i)$, for $i = 0, 1$, is defined in Proposition 3, and $Q(\cdot)$ is the Q-function. In order to find $\boldsymbol{\rho}^\star$, we have the following optimization problem:

$$\boldsymbol{\rho}^\star = \underset{\boldsymbol{\rho}\in[0,1]^M}{\arg\min} \left(P_0 P_\mathrm{F} + P_1 P_\mathrm{M}\right). \tag{19}$$

The necessary conditions of $\boldsymbol{\rho}^\star$ in (19) are derived in the proposition below.

Proposition 4 (Necessary conditions of $\boldsymbol{\rho}^\star$) *The transmission probabilities* $\boldsymbol{\rho}^\star = (\rho_1^\star, \rho_2^\star, \ldots, \rho_M^\star)$ *in* (19) *must satisfy the following conditions:*

(i) *Let* $g_m(\rho_m)$ *be a function of* ρ_m *defined as*

$$\frac{\frac{(1-\bar{p}_{\mathrm{C},m|0})^2}{2\bar{p}_{\mathrm{C},m|0}(1-\bar{p}_{\mathrm{C},m|0})-(1-\bar{n}_{m|0})\bar{p}_{\mathrm{S},m|0}\left[\log\left(1-\frac{\rho_m}{K}\right)\right]}}{\frac{(1-\bar{p}_{\mathrm{C},m|1})^2}{2\bar{p}_{\mathrm{C},m|1}(1-\bar{p}_{\mathrm{C},m|1})-(1-\bar{n}_{m|1})\bar{p}_{\mathrm{S},m|1}\left[\log\left(1-\frac{\rho_m}{K}\right)\right]}}, \tag{20}$$

for all m, *where* $\bar{n}_{m|i}$, $\bar{p}_{\mathrm{S},m|i}$, *and* $\bar{p}_{\mathrm{C},m|i}$ *are defined in Proposition* 3. *We have*

$$g_1(\rho_1^\star) = g_2(\rho_2^\star) = \ldots = g_M(\rho_M^\star). \tag{21}$$

(ii) *The function* $g_m(\rho_m^\star)$, *for all* m, *must be equal to*

$$\left(\frac{\sigma_1^\star}{\sigma_0^\star}\right)^3\left[\frac{P_0\varphi\left(\frac{\gamma-\mu_0}{\sigma_0^\star}\right)(\gamma-\mu_0)}{P_1\varphi\left(\frac{\gamma-\mu_1}{\sigma_1^\star}\right)(\gamma-\mu_1)}\right], \tag{22}$$

where $\varphi(\cdot)$ *is the standard Gaussian PDF and* $\sigma_i^\star$ *is the standard deviation* σ_i *in* (16) *with substituting* $\boldsymbol{\rho}^\star = (\rho_1^\star, \rho_2^\star, \ldots, \rho_M^\star)$.

(iii) *With properly choosing* γ *such that* $\mu_0 \le \gamma \le \mu_1$, *the value* $g_m(\rho_m^\star)$ *is less than or equal to zero for all* m.

Proof Please see Appendix D. □

The necessary conditions in Proposition 4 help us in searching for the transmission probabilities $\boldsymbol{\rho}^\star$. First, we can find a range of feasible values of $\rho_m^\star$ by using the necessary conditions (i) and (iii). Thereafter, we limit to specific candidates of ρ_m^* by using the necessary condition (ii). An example of finding the transmission probabilities $\boldsymbol{\rho}^\star = (\rho_1^\star, \rho_2^\star, \ldots, \rho_M^\star)$ is explained below.

Example 1 Consider the observation x governed by the following binary hypothesis testing model

$$H_0: \ x \sim \mathcal{N}(0,5) \quad \text{and} \quad H_1: \ x \sim \mathcal{N}(1,5), \tag{23}$$

where $\mathcal{N}(a,b)$ is the Gaussian PDF whose mean and variance are equal to a and b, respectively. Assume further that $P_0 = P_1 = \frac{1}{2}$ and $N = 400$. We consider the proposed distributed detection when $T = 80$, $M = 4$, $K = 20$, and $\gamma = \frac{1}{2}$. The observation range is divided into one censored region:

$$\mathcal{C}_1 = \{x : 0 < x \le 1\}, \tag{24}$$

and four uncensored regions:

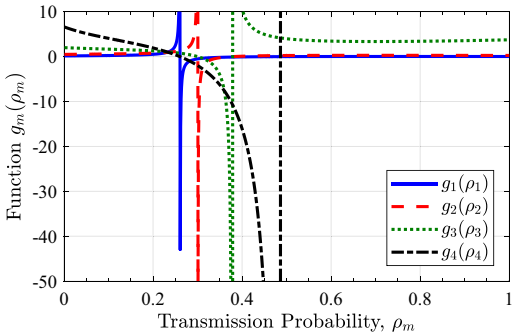

a A plot of the function $g_m(\rho_m)$ defined in (20), for $m = 1, 2, 3, 4$. Since we are interested in the region where $g_m(\rho_m) \leq 0$ (the necessary condition (iii)), only the values of $-50 \leq g_m(\rho_m) \leq 10$ are shown.

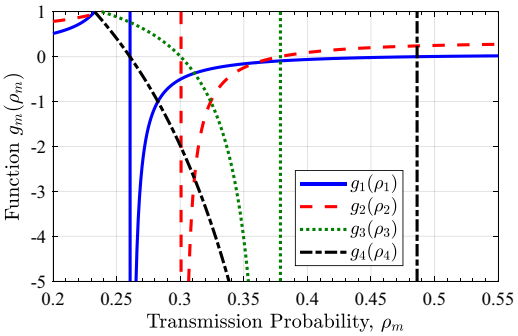

b We take a close-up of the plot shown in Fig. 6(a) to show the points whose $g_m(\rho_m) = 0$, for all m. We, then, can find the feasible values of $\rho_m^\star$ as follows. Consider a plot of $g_1(\rho_1)$. We have $g_1(\rho_1) \leq 0$ for $0.261 \leq \rho_1 \leq 0.486$, which is the feasible region of $\rho_1^\star$. The feasible regions of $\rho_2^\star$, $\rho_3^\star$, and $\rho_4^\star$ can be found in the same way. Furthermore, as explained in Example 2, we notice that $g_1(\rho_1)$ and $g_4(\rho_4)$ cross each other when their values are -1. The corresponding ρ_m is the optimal transmission probability for $m = 1$ and $m = 4$. For $g_2(\rho_2)$ and $g_3(\rho_3)$, we have the same observations.

Fig. 6 Illustrations of Examples 1 and 2

$$\begin{aligned}
\mathcal{U}_1 &= \{x : -\infty < x \leq -1.385\},\\
\mathcal{U}_2 &= \{x : -1.385 < x \leq 0\},\\
\mathcal{U}_3 &= \{x : 1 < x \leq 2.385\},\\
\mathcal{U}_4 &= \{x : 2.385 < x < \infty\}.
\end{aligned} \tag{25}$$

Note that the thresholds in the uncensored regions are selected such that the probability $q_{m|0}P_0 + q_{m|1}P_1$, for $m = 1, 2, 3, 4$, are identical (specifically, $q_{m|0}P_0 + q_{m|1}P_1 = \frac{1-(P_0 q_{M+1|0} + P_1 q_{M+1|1})}{M}$). The function $g_m(\rho_m)$ defined in (20), for $m = 1, 2, 3, 4$, are shown in Fig. 6a. Only the negative values are displayed because of the necessary condition (iii). From (21) and the fact that $g_m(\rho_m^*) \leq 0$, for all m, Fig. 6b shows that the feasible values of $\rho_1^\star$, $\rho_2^\star$, $\rho_3^\star$, and $\rho_4^\star$ are

$$\begin{aligned}
0.261 \leq \rho_1^\star \leq 0.486, \quad 0.301 \leq \rho_2^\star \leq 0.379,\\
0.301 \leq \rho_3^\star \leq 0.379, \quad 0.261 \leq \rho_4^\star \leq 0.486.
\end{aligned}$$

To find the transmission probabilities $\rho_1^\star$, $\rho_2^\star$, $\rho_3^\star$, and $\rho_4^\star$, we vary ρ_1, ρ_2, ρ_3, and ρ_4 within the feasible ranges identified above such that the necessary condition (ii) is true. The corresponding transmission probabilities $\boldsymbol{\rho}^\star = (\rho_1^\star, \rho_2^\star, \rho_3^\star, \rho_4^\star)$ minimize the probability of error in (19). As a result, we obtain $\rho_1^\star = 0.282$, $\rho_2^\star = 0.324$, $\rho_3^\star = 0.324$, and $\rho_4^\star = 0.282$. □

A feasible region of $\rho_m^\star$ as shown in the example above can be determined in the following way.

Proposition 5 (A feasible region of $\rho_m^\star$) *The optimal transmission probabilities $\rho_m^\star$ is between $\rho_{m|0}^\star$ and $\rho_{m|1}^\star$, where $\rho_{m|i}^\star$ is obtained from*

$$\frac{(1-\bar{p}_{\mathrm{C},m|i}^\star)\bar{p}_{\mathrm{C},m|i}^\star}{\bar{p}_{\mathrm{S},m|i}^\star} = \frac{(1-\bar{n}_{m|i})}{2}\left[\log\left(1-\frac{\rho_{m|i}^\star}{K}\right)\right], \tag{26}$$

$\bar{p}_{\mathrm{C},m|i}^\star = 1-\bar{p}_{0,m|i}^\star-\bar{p}_{\mathrm{S},m|i}^\star$, $\bar{p}_{0,m|i}^\star = \left(1-\frac{\rho_{m|i}^\star}{K}\right)^{\bar{n}_{m|i}}$, *and* $\bar{p}_{\mathrm{S},m|i}^\star = \bar{n}_{m|i}\left(\frac{\rho_{m|i}}{K}\right)\left(1-\frac{\rho_{m|i}}{K}\right)^{\bar{n}_{m|i}-1}$. *The transmission probabilities* $\rho_{1|0}^\star, \rho_{2|0}^\star, \cdots, \rho_{M|0}^\star$ *minimize the probability of false alarm* P_{F}. *The transmission probabilities* $\rho_{1|1}^\star, \rho_{2|1}^\star, \cdots, \rho_{M|1}^\star$ *minimize the probability of miss* P_{M}.

Proof Please see Appendix E. □

Consider Example 1. We find the transmission probabilities $\rho_{1|0}^\star$ and $\rho_{1|1}^\star$ by using (26). As a result, we have $\rho_{1|0}^\star = 0.261$ and $\rho_{1|1}^\star = 0.486$. From Proposition 5, the feasible region of $\rho_1^\star$ is $0.261 \le \rho_1^\star \le 0.486$, which is similar to that specified in Example 1.

The transmission probabilities $\boldsymbol{\rho}^\star = (\rho_1^\star, \rho_2^\star, \ldots, \rho_M^\star)$ are easily found when the following conditions are true.

Corollary 2 (Special case) *Assume M is even, the threshold $\gamma = \frac{1}{2}(\mu_0+\mu_1)$, and $q_{m|0} = q_{M+1-m|1}$ for all m. The transmission probabilities $\boldsymbol{\rho}^\star = (\rho_1^\star, \rho_2^\star, \ldots, \rho_M^\star)$ in (19) must satisfy the following conditions*:

(i) *The optimal transmission probabilities satisfy*

$$\rho_m^\star = \rho_{M+1-m}^\star, \quad \forall m. \tag{27}$$

(ii) *The function $g_m(\rho_m^\star)$ defined in (20) must be equal to $-\frac{P_0}{P_1}$, for all m.*

Proof First, we can prove the condition (i) as follows. From the given assumption that $q_{m|0} = q_{M+1-m|1}$, we have $\bar{n}_{m|0} = \bar{n}_{M+1-m|1}$, where $\bar{n}_{m|i} = Nq_{m|i}$. Recall that the function $g_m(\rho_m)$ defined in (20) is a function of $\bar{n}_{m|0}$, $\bar{n}_{m|1}$, and ρ_m. Since $\bar{n}_{m|0} = \bar{n}_{M+1-m|1}$ and $g_m(\rho_m^\star) = g_{M+1-m}(\rho_{M+1-m}^\star)$ from (21), we have $\rho_m^\star = \rho_{M+1-m}^\star$ for all m.

Second, we can prove the condition (ii) as follows. Since M is even, $q_{m|0} = q_{M+1-m|1}$, $\bar{n}_{m|i} = Nq_{m|i}$, and $\rho_m^\star = \rho_{M+1-m}^\star$, we have $\mu_0 = -\mu_1$ and $\sigma_0^\star = \sigma_1^\star$, where μ_i and σ_i^2 are defined in (15) and (16), respectively. Recall that $\sigma_i^\star$ is the standard deviation σ_i in (16) with substituting $\boldsymbol{\rho}^\star = (\rho_1^\star, \rho_2^\star, \ldots, \rho_M^\star)$. In addition, from the given assumption that $\gamma = \frac{1}{2}(\mu_0 + \mu_1)$, we have $\gamma = 0$. As considering (22), we have $(\gamma - \mu_0) = -(\gamma - \mu_1)$ and $\varphi\left(\frac{\gamma-\mu_0}{\sigma_0^\star}\right) = \varphi\left(\frac{\gamma-\mu_1}{\sigma_1^\star}\right)$. As a result, (22) is reduced to $-\frac{P_0}{P_1}$, which is the value of $g_m(\rho_m^\star)$. □

The example below shows how easy to find the optimal transmission probabilities $\boldsymbol{\rho}^\star$ when the assumptions in Corollary 2 are true.

Example 2 Reconsider Example 1. We can see that the parameter setup in Example 1 follows the assumptions in Corollary 2. From Corollary 2, we will have $\rho_1^\star = \rho_4^\star$, $\rho_2^\star = \rho_3^\star$, and $g_m(\rho_m^\star) = -1$, for all m. Considering Fig. 6b, we obtain $\rho_1^\star = 0.282$, $\rho_2^\star = 0.324$, $\rho_3^\star = 0.324$, and $\rho_4^\star = 0.282$. □

5 Results and discussion

In this section, we will evaluate and show the performance of the collision-aware distributed detection with the PSRA. Throughout this section, we assume that the observation x is governed by the model shown in (23) in Example 1 whose observation signal-to-noise ratio (SNR) is equal to −7 dB. As a result, according to [9], the reliability of the observation will be equal to $|x - 0.5|$. The value of x that is further away from 0.5 is more reliable. Therefore, as seen later, our censored regions (cover unreliable observations) will be around $x = 0.5$. Note that the probabilities of error P_E shown in this section are obtained from simulation and the probabilities P_0 and P_1 are equal to $\frac{1}{2}$.

5.1 Network traffic and optimal transmission probabilities

In a data network using slotted ALOHA, the optimal transmission probability will be the probability that maximizing the network throughput (i.e., the probability of successful transmission) [31]. However, in this paper, our optimal transmission probabilities $\boldsymbol{\rho}^* = (\rho_1^*, \rho_2^*, \ldots, \rho_M^*)$ are to minimize the proposed distributed detection's error probability P_E. We study the role of the transmission probabilities on the probability of error P_E in the following scenario. We consider a distributed detection system with 500 sensor nodes. The collection time T is equal to 30 time slots, which is divided into two frames. Each frame consists of 15 time slots. The observation range is divided into one censored region $\mathcal{C}_1 = \{x : -1 < x \leq 2\}$ and two uncensored regions $\mathcal{U}_1 = \{x : -\infty < x \leq -1\}$ and $\mathcal{U}_2 = \{x : 2 < x < \infty\}$. We have $q_{1|0} = q_{2|1}$ and $q_{1|1} = q_{2|0}$. The probability that the event H_i (i.e., P_i) happens is equal to $\frac{1}{2}$. As a result, we have $P_0 q_{1|0} + P_1 q_{1|1} = P_0 q_{2|0} + P_1 q_{2|1}$.

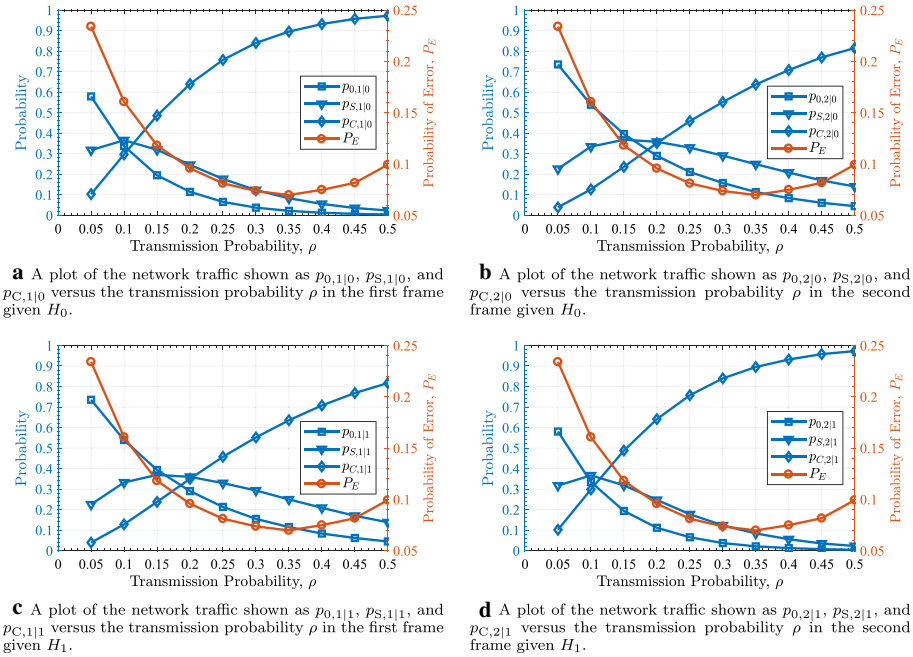

a A plot of the network traffic shown as $p_{0,1|0}$, $p_{S,1|0}$, and $p_{C,1|0}$ versus the transmission probability ρ in the first frame given H_0.

b A plot of the network traffic shown as $p_{0,2|0}$, $p_{S,2|0}$, and $p_{C,2|0}$ versus the transmission probability ρ in the second frame given H_0.

c A plot of the network traffic shown as $p_{0,1|1}$, $p_{S,1|1}$, and $p_{C,1|1}$ versus the transmission probability ρ in the first frame given H_1.

d A plot of the network traffic shown as $p_{0,2|1}$, $p_{S,2|1}$, and $p_{C,2|1}$ versus the transmission probability ρ in the second frame given H_1.

Fig. 7 Simulation results showing the role of the transmission probability on the proposed distributed detection's network traffic and probability of error P_E. The parameters are set up as follows: $N = 500, T = 30$, $M = 2$, and $K = 15$. The range of the observation is divided into a censored region $\mathcal{C}_1 = \{x : -1 < x \leq 2\}$ and two uncensored regions $\mathcal{U}_1 = \{x : -\infty < x \leq -1\}$ and $\mathcal{U}_2 = \{x : 2 < x < \infty\}$

According to the parameter setup above, the transmission probability ρ_1^* will be equal to the transmission probability ρ_2^*. Therefore, we vary the transmission probability ρ_m such that $\rho_1 = \rho_2 = \rho$. From simulations, the probability of error P_E versus ρ is shown in Fig. 7. In addition, we show the network traffic (which is measured by $p_{0,m|i}$, $p_{S,m|i}$, and $p_{C,m|i}$) versus ρ for $m = 1, 2$ and $i = 0, 1$ in Fig. 7a–d. We can see that the transmission probabilities minimizing P_E are $\rho_1^* = \rho_2^* \approx 0.33$. We further notice that the optimal transmission probabilities $\boldsymbol{\rho^*} = (\rho_1^*, \rho_2^*, \ldots, \rho_M^*)$ do not maximize the network throughput (i.e., $p_{S,m|i}$). However, by using the optimal transmission probabilities $\boldsymbol{\rho^*} = (\rho_1^*, \rho_2^*, \ldots, \rho_M^*)$, a lot of collisions occur (i.e., high $p_{C,m|i}$) in each frame. A reason is that, unlike the sensor networks whose collisions are non-informative and, then, neglected [7–9, 20, 31], in the proposed distributed detection, the collision time slots can be exploited in making a final decision.

Next, we show the optimal transmission probabilities $\boldsymbol{\rho^*} = (\rho_1^*, \rho_2^*, \ldots, \rho_M^*)$ (minimizing the probability P_E) when increasing N in Fig. 8. The same scenario described above is assumed except the value of N. Since ρ_1^* is equal to ρ_2^*, only ρ_1^* is shown. Increasing N means that there are more sensor nodes in each uncensored region $\mathcal{R}_m$. Recall that these sensor nodes will send their data bits in the mth frame with the transmission probability ρ_m. The number N and the probability ρ_m will affect to the numbers of time-slot states $(z_{0,m}, z_{S,m}, z_{C,m})$. For a fixed ρ_m, increasing N will result in higher collision time slots $z_{C,m}$ and lower idle time slots $z_{0,m}$. The proposed scheme exploits the numbers of time-slot states $(z_{0,m}, z_{S,m}, z_{C,m})$ to differentiate between the event H_0 and the event H_1.

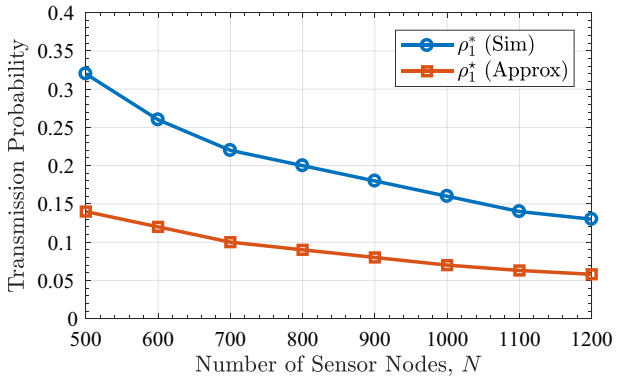

Fig. 8 A comparison between the optimal transmission probability ρ_1^* obtained from simulations and the approximation $\rho_1^\star$ obtained from Proposition 4. The parameters are set up as follows: $T = 30$, $M = 2$, and $K = 15$. The range of the observation is divided into a censored region $\mathcal{C}_1 = \{x : -1 < x \leq 2\}$ and two uncensored regions $\mathcal{U}_1 = \{x : -\infty < x \leq -1\}$ and $\mathcal{U}_2 = \{x : 2 < x < \infty\}$

As a result, increasing N lowers the optimal transmission probability ρ_1^* such that the corresponding time-slot states $(z_{0,m}, z_{S,m}, z_{C,m})$ are best used in detection.

In addition, we also show the transmission probability $\rho_1^\star$, which is an approximation of the optimal transmission probability ρ_1^*, versus N in Fig. 8. The probability $\rho_1^\star$ is easily obtained from Proposition 4. We see that there is an acceptable gap between ρ_1^* and $\rho_1^\star$, which is smaller when increasing N.

5.2 Performance comparison

In this section, we demonstrate

- the estimated number of sensor nodes $\hat{n}_m$ obtained from the population estimator (10),
- the effect of N on the probability of error P_E of the proposed distributed detection scheme,
- the effect of censored regions on the probability of error P_E of the proposed distributed detection scheme.

However, finding the optimal transmission probabilities $\boldsymbol{\rho}^* = (\rho_1^*, \rho_2^*, \ldots, \rho_M^*)$ is cumbersome. Therefore, we will find the transmission probabilities $\boldsymbol{\rho}^\star = (\rho_1^\star, \rho_2^\star, \ldots, \rho_M^\star)$, which can be obtained from Proposition 4, and use them instead.

Figure 9 compares the estimated number of sensor nodes $\hat{n}_m$ obtained from (10) with the actual number of sensor nodes n_m in the mth frame for 50 trials when $M = 2$, $T = 60$, $K = 30$, and $N = 500$. We assume that the event H_1 is happening. The other parameters are specified in the figure's caption. We see that the estimate $\hat{n}_m$ has fluctuated around the actual number n_m.

Figure 10 shows the effect of N on the proposed distributed detection (specified as PSRA) when $M = 2$ and $M = 6$. The parameter setup is specified in the figure's caption. Recall that for a given K (the number of time slots in each frame), there will be a set of

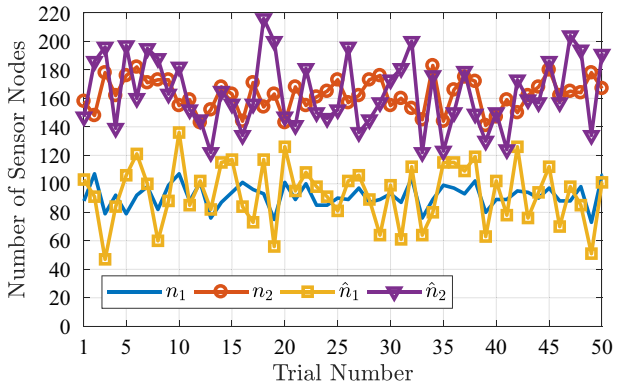

Fig. 9 A comparison between the estimated number of sensor nodes $\hat{n}_m$ and the actual number of sensor nodes n_m in the mth frame for 50 trials when $M = 2$, $T = 60$, $K = 30$, and $N = 500$. We assume that the event H_1 is happening. The range of the observation is divided into a censored region $\mathcal{C}_1 = \{x : -1 < x \leq 2\}$ and two uncensored regions $\mathcal{U}_1 = \{x : -\infty < x \leq -1\}$ and $\mathcal{U}_2 = \{x : 2 < x < \infty\}$. As a result, we have $q_{m|0}P_0 + q_{m|1}P_1$, for $1 \leq m \leq 2$, are identical. The approximations of the optimal transmission probabilities $\boldsymbol{\rho}^\star = (\rho_1^\star, \rho_2^\star)$ are obtained from Proposition 4, where we have $\rho_1^\star = \rho_2^\star = 0.28$

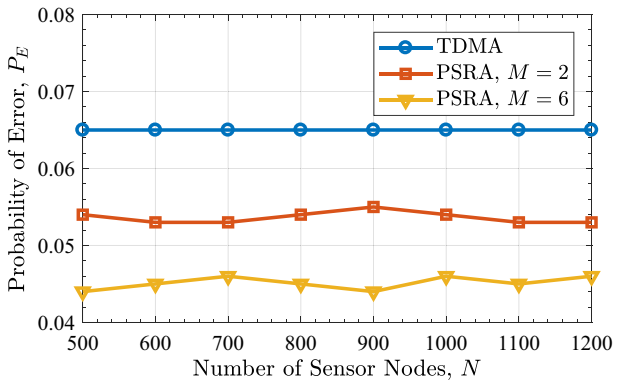

Fig. 10 Simulation results showing the probability of error P_E of the proposed distributed detection versus N. In addition, we compare the probability of error P_E of the proposed distributed detection (specified as PSRA) to the distributed detection using TDMA (specified as TDMA). The parameters are set up as follows. The collection time T is equal to 60 time slots. The number of frames (M) is specified in the figure. The approximations of the optimal transmission probabilities $\boldsymbol{\rho}^\star = (\rho_1^\star, \rho_2^\star, \ldots, \rho_M^\star)$ from Proposition 4 are applied. The range of the observation is divided into a censored region $\mathcal{C}_1 = \{x : -1 < x \leq 2\}$ and M uncensored regions $\mathcal{U}_1, \mathcal{U}_2, \cdots, \mathcal{U}_M$. The thresholds of $\mathcal{U}_m$ which are τ_m^L and τ_m^U, are selected such that $q_{m|0}P_0 + q_{m|1}P_1$, for all m, are identical

$z_{0,m}$, $z_{\mathrm{S},m}$, and $z_{\mathrm{C},m}$ that are best used in differentiating between the event H_0 and the event H_1. Increasing N will introduce higher number of sensor nodes in each observation interval. The transmission probabilities $\boldsymbol{\rho} = (\rho_1, \rho_2, \ldots, \rho_M)$ are used to adjust the number $z_{0,m}$, $z_{\mathrm{S},m}$, and $z_{\mathrm{C},m}$, which will be further exploited by the FC to make a final decision. By using the transmission probabilities $\boldsymbol{\rho}^\star = (\rho_1^\star, \rho_2^\star, \ldots, \rho_M^\star)$, a set of suitable $z_{0,m}$, $z_{\mathrm{S},m}$, and $z_{\mathrm{C},m}$ will be seen by the fusion center. This is roughly independent on N. Therefore, increasing N slightly affects the probability P_E.

In Fig. 10, we also show the probability of error P_E of the distributed detection using a time division multiple access (TDMA) protocol. In the TDMA protocol, each sensor node is assigned a specific time slot to send its data in advance to avoid packet

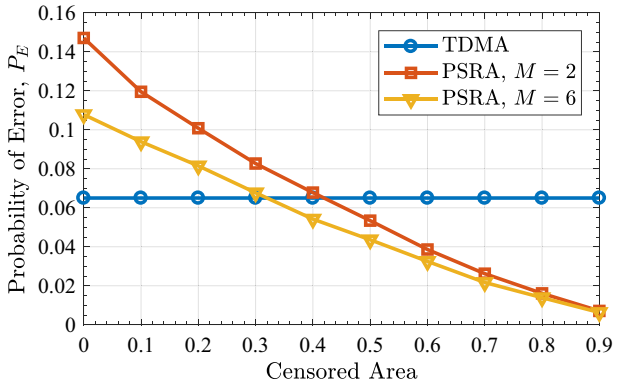

Fig. 11 Simulation results showing the probability of error P_{E} of the proposed distributed detection versus the censored area (which is equal to $P_0 q_{M+1|0} + P_1 q_{M+1|1}$). In addition, we compare the probability of error P_{E} of the proposed distributed detection (specified as PSRA) to the distributed detection using TDMA (specified as TDMA). The parameters are set up as follows: $N = 800$ and $T = 60$. The number of frames (M) is specified in the figure. The approximations of the optimal transmission probabilities $\boldsymbol{\rho}^{\star} = (\rho_1^{\star}, \rho_2^{\star}, \ldots, \rho_M^{\star})$ from Proposition 4 are applied. The range of the observation is divided into a censored region $\mathcal{C}_1 = \{x :< \nu_1^L < x \leq \nu_1^U\}$ and M uncensored regions $\mathcal{U}_1, \mathcal{U}_2, \cdots, \mathcal{U}_M$. The thresholds of $\mathcal{C}_1$, which are ν_1^L and ν_1^U, are adjusted to get the desired censored area. The thresholds of $\mathcal{U}_m$ which are τ_m^L and τ_m^U, are selected such that $q_{m|0}P_0 + q_{m|1}P_1$, for all m, are identical

collisions. In our scenario, since $T < N$, a group of 60 sensor nodes are randomly selected and assigned exclusive time slots to send their local decisions. The local decision is computed as follows: if the observation x is larger than 0.5 (i.e., the local threshold obtained from our scenario assumption), the local decision is one; otherwise, the local decision is zero. The FC receives 60 local decisions without collisions and sums them together to compute its test statistic. If the test statistic is larger than zero, the FC announces the event H_1; otherwise, the FC announces the event H_0. As shown in the figure, the corresponding probability P_{E} of the TDMA-based distributed detection is about 0.0647, which is higher than that of the proposed distributed detection.

Figure 11 shows the effect of the censored area on the proposed distributed detection (specified as PSRA) when $M = 2$ and $M = 6$. Increasing the censored area indicates that only data bits obtained from *higher reliable* observations will be sent to the FC (and, as a result, lowers the number of sensor nodes who will send their data bits to the FC). The censored area is computed from $P_0 q_{M+1|0} + P_1 q_{M+1|1}$. In this figure, we consider that the range of the observation is divided into a censored region $\mathcal{C}_1 = \{x : \nu_1^L < x \leq \nu_1^U\}$ and M uncensored regions. The value of $q_{M+1|i}$ is obtained from $\int_{\nu_1^L}^{\nu_1^U} f_X(x|H_i)\, dx$. We set the thresholds $\nu_1^L = 0.5 - a$ and $\nu_1^U = 0.5 + a$, for $a > 0$, and vary a to get the desired censored area. The other parameters are set up as shown in the figure's caption. We see that increasing the censored area such that only data bits obtained from reliable observations are sent to the FC significantly helps improving the probability of error P_{E}. We also show the probability P_{E} of the TDMA-based distributed detection for a comparison. The proposed distributed detection outperforms the TDMA-based distributed detection when the censored area is larger than 0.42 and 0.32 for $M = 2$ and $M = 6$, respectively.

6 Conclusions

We have proposed a collision-aware distributed detection scheme with the PSRA for a single-hop WSN whose collection time is limited and only a collision channel between sensor nodes and the FC is provided. We have shown that, unlike many other random-access distributed detection schemes, the proposed distributed detection favors a large number of collision time slots since the collisions are useful and applicable in making a final decisions. The following are possible extensions of the proposed distributed detection such that its performance is improved and/or it is applied in other scenarios.

i. *Composite Hypothesis Testing:* In this paper, we assume that the distributions of the observation given H_0 and H_1 are known and we, then, formulate the problem as simple binary hypothesis testing. However, in many scenarios, for example, the distribution of the observation given H_1 generally is unknown since its distribution would depend on the location and the strength of the event. Study, analysis, and evaluation of the proposed distributed detection in the composite hypothesis testing is an interesting extension.
ii. *Energy Detection:* In this paper, we design and analyze the proposed distributed detection by assuming that the FC is able to detect the time slot states: idle, successful, and collision time slots. A method to identify these time slot states are open. Specifically, what we study here is from the MAC layer's point of view. We can extend the proposed distributed detection towards the physical layer's point of view by including an energy detection into the proposed distributed detection to detect the time slot states. Furthermore, we, then, are able to investigate the effect of the fading channels on the proposed distributed detection.

Appendix A: Proof of Proposition 1

The ML estimate of the variable n_m, $\hat{n}_m$ as shown in (10), is directly obtained from (7). For a large K, the distribution of the estimate $\hat{n}_m$ asymptotically converges to a Gaussian distribution $\mathcal{N}\left(n_m, \upsilon_m^2\right)$, where υ_m^2 is equal to the Cramer-Rao lower bound of $\hat{n}_m$ [3].

To derive the variance υ_m^2, we omit the fact that n_m is an integer and, then, consider n_m as a real number. The variance υ_m^2 is obtained from

$$\upsilon_m^2 = \frac{1}{-\mathbb{E}\left\{\frac{\partial^2}{\partial n_m^2}\log \Pr(\mathbf{z}_m|n_m)\right\}}. \tag{28}$$

The first derivative $\frac{\partial}{\partial n_m}\log \Pr(\mathbf{z}_m|n_m)$ and the second derivative $\frac{\partial^2}{\partial n_m^2}\log \Pr(\mathbf{z}_m|n_m)$ are shown as follows:

$$\begin{aligned}\frac{\partial}{\partial n_m}\log\Pr(\mathbf{z}_m|n_m) &= z_{0,m}\log\left(1-\frac{\rho_m}{K}\right)\\ &\quad + z_{\mathrm{S},m}\left[\log\left(1-\frac{\rho_m}{K}\right)+\frac{1}{n_m}\right]\\ &\quad + z_{\mathrm{C},m}\left[\left(\frac{p_{\mathrm{C},m}-1}{p_{\mathrm{C},m}}\right)\log\left(1-\frac{\rho_m}{K}\right)-\frac{p_{\mathrm{S},m}}{n_m p_{\mathrm{C},m}}\right],\end{aligned} \tag{29}$$

$$\begin{aligned}\frac{\partial^2}{\partial n_m^2}\log\Pr(\mathbf{z}_m|n_m) &= \frac{z_{\mathrm{C},m}(p_{\mathrm{C},m}-1)}{p_{\mathrm{C},m}^2}\left[\log\left(1-\frac{\rho_m}{K}\right)\right]^2\\ &\quad - \frac{z_{\mathrm{C},m}p_{\mathrm{S},m}}{n_m p_{\mathrm{C},m}}\left[1+\left(\frac{2-p_{\mathrm{C},m}}{p_{\mathrm{C},m}}\right)\right]\log\left(1-\frac{\rho_m}{K}\right)\\ &\quad - \frac{1}{n_m^2}\left[z_{\mathrm{S},m}+\frac{z_{\mathrm{C},m}p_{\mathrm{S},m}^2}{p_{\mathrm{C},m}^2}\right].\end{aligned} \tag{30}$$

Because of $\mathbb{E}\{z_{\mathrm{S},m}\} = Kp_{\mathrm{S},m}$ and $\mathbb{E}\{z_{\mathrm{C},m}\} = Kp_{\mathrm{C},m}$, we have

$$\begin{aligned}\mathbb{E}\left\{\frac{\partial^2}{\partial n_m^2}\log\Pr(\mathbf{z}_m|n_m)\right\} &= K\left(\frac{p_{\mathrm{C},m}-1}{p_{\mathrm{C},m}}\right)\left[\log\left(1-\frac{\rho_m}{K}\right)\right]^2\\ &\quad - \frac{Kp_{\mathrm{S},m}}{n_m}\left[1+\left(\frac{2-p_{\mathrm{C},m}}{p_{\mathrm{C},m}}\right)\right]\log\left(1-\frac{\rho_m}{K}\right)\\ &\quad - \frac{Kp_{\mathrm{S},m}}{n_m^2}\left(1+\frac{p_{\mathrm{S},m}}{p_{\mathrm{C},m}}\right).\end{aligned} \tag{31}$$

By assuming that n_m is large and $n_m \gg K$, the term $\mathbb{E}\{\frac{\partial^2}{\partial n_m^2}\log\Pr(\mathbf{z}_m|n_m)\}$ can be approximated as

$$\mathbb{E}\left\{\frac{\partial^2}{\partial n_m^2}\log\Pr(\mathbf{z}_m|n_m)\right\} \approx K\left(\frac{p_{\mathrm{C},m}-1}{p_{\mathrm{C},m}}\right)\left[\log\left(1-\frac{\rho_m}{K}\right)\right]^2. \tag{32}$$

Since $p_{\mathrm{C},m}$ is less than or equal to one, the term $(p_{\mathrm{C},m}-1)$ is a negative value. By substituting (32) into (28), we obtain (11).

Appendix B: Proof of Corollary 1

Note that we assume n_m is real-valued. Consider the derivatives $\frac{\partial}{\partial n_m}\log\Pr(\mathbf{z}_m|n_m)$ and $\frac{\partial^2}{\partial n_m^2}\log\Pr(\mathbf{z}_m|n_m)$ shown in (29) and (30), respectively. For a large n_m, these derivatives can be approximated as

$$\frac{\partial}{\partial n_m}\log\Pr(\mathbf{z}_m|n_m) \approx \left[z_{0,m}+z_{\mathrm{S},m}+\left(\frac{p_{\mathrm{C},m}-1}{p_{\mathrm{C},m}}\right)z_{\mathrm{C},m}\right]\times\log\left(1-\frac{\rho_m}{K}\right), \tag{33}$$

$$\frac{\partial^2}{\partial n_m^2}\log\Pr(\mathbf{z}_m|n_m) \approx z_{\mathrm{C},m}\left(\frac{p_{\mathrm{C},m}-1}{p_{\mathrm{C},m}^2}\right)\left[\log\left(1-\frac{\rho_m}{K}\right)\right]^2. \tag{34}$$

Since $\left(\frac{p_{C,m}-1}{p_{C,m}^2}\right) \leq 0$, we have $\frac{\partial^2}{\partial n_m^2} \log \Pr(\mathbf{z}_m|n_m) \leq 0$, which means the term $\log \Pr(\mathbf{z}_m|n_m)$ is a concave function of n_m. Therefore, the ML estimate $\hat{n}_m$ is the value n_m satisfying $\frac{\partial}{\partial n_m} \log \Pr(\mathbf{z}_m|n_m) = 0$, which is equivalent to

$$z_{0,m} + z_{S,m} + \left(\frac{p_{C,m}-1}{p_{C,m}}\right) z_{C,m} = 0. \tag{35}$$

Recall the $z_{0,m} + z_{S,m} = K - z_{C,m}$. Therefore, we have (12).

Appendix C: Proof of Proposition 3

The test statistic Λ can be rewritten as $\Lambda = \sum_{m=1}^{M} \Lambda_m$, where

$$\Lambda_m = \hat{n}_m \left[\log\left(\frac{q_{m|1}}{q_{M+1|1}}\right) - \log\left(\frac{q_{m|0}}{q_{M+1|0}}\right)\right]. \tag{36}$$

From Proposition 1, where $\hat{n}_m \overset{a}{\sim} \mathcal{N}(n_m, \upsilon_m^2)$, the conditional PDF of Λ_m given n_m (i.e., $\Pr(\Lambda_m|n_m)$) is asymptotically equal to $\mathcal{N}(\eta_m, \vartheta_m^2)$, where

$$\eta_m = n_m \left[\log\left(\frac{q_{m|1}}{q_{M+1|1}}\right) - \log\left(\frac{q_{m|0}}{q_{M+1|0}}\right)\right], \tag{37}$$

$$\vartheta_m^2 = \upsilon_m^2 \left[\log\left(\frac{q_{m|1}}{q_{M+1|1}}\right) - \log\left(\frac{q_{m|0}}{q_{M+1|0}}\right)\right]^2. \tag{38}$$

Given $\mathbf{n} = (n_1, n_2, \ldots, n_M)$, the test statistics $\Lambda_1, \Lambda_2, \cdots, \Lambda_M$ are independent. The conditional PDF of Λ given $\mathbf{n}$ can be expressed as $\Pr(\Lambda|\mathbf{n}) = \prod_{m=1}^{M} \Pr(\Lambda_m|n_m)$. We have $\Pr(\Lambda|H_i) = \mathbb{E}_{\mathbf{n}}\left\{ \prod_{m=1}^{M} \Pr(\Lambda_m|n_m) \middle| H_i \right\}$.

Since we would like to find $\Pr(\Lambda|H_i)$ in a closed form, an approximation will be conducted. By using the Demoivre-Laplace theorem, the conditional PDF $\Pr(\mathbf{n}|H_i)$ is approximated as $\tilde{\Pr}(\mathbf{n}|H_i)$ which is expressed as $\prod_{m=1}^{M} \frac{1}{\sqrt{2\pi\varsigma_{m|i}^2}} e^{-\frac{(n_m - \bar{n}_{m|i})^2}{2\varsigma_{m|i}^2}}$, where $\bar{n}_{m|i} = Nq_{m|i}$ and $\varsigma_{m|i}^2 = Nq_{m|i}(1-q_{m|i})$. As a result, we can approximate $\Pr(\Lambda|H_i)$ as $\tilde{\Pr}(\Lambda|H_i) = \prod_{m=1}^{M} \tilde{\Pr}(\Lambda_m|H_i)$, where

$$\tilde{\Pr}(\Lambda_m|H_i) = \int_{-\infty}^{\infty} \Pr(\Lambda_m|n_m)\, \tilde{\Pr}(n_m|H_i)\, dn_m. \tag{39}$$

Similar to the proof shown in Appendix A of [43], by applying Gauss-Hermite quadrature integration, we can show that

$$\tilde{\Pr}(\Lambda_m|H_i) \approx \frac{1}{\sqrt{\pi}} \sum_{j=1}^{J} C_j \Pr\left(\Lambda_m \middle| n_m\right)\Big|_{n_m = \bar{n}_{m|i} + \sqrt{2} r_j \varsigma_{m|i}}, \tag{40}$$

where J is the number of sample points, r_j is the jth root of Hermite polynomial, and C_j is the associated weight of the jth root. By using $J = 1$, where $r_1 = 0$ and $C_1 = \sqrt{\pi}$, we

have $\tilde{\Pr}(\Lambda_m|H_i) \approx \Pr(\Lambda_m|n_m)\big|_{n_m=\bar{n}_{m|i}}$. As a result, we obtain an approximation of the conditional PDF of Λ given H_i as shown in Proposition 3.

Appendix D: Proof of Proposition 4

The necessary condition for the optimal transmission probabilities $\boldsymbol{\rho}^\star$ in (19) is that the function $\frac{\partial}{\partial\rho_m}\left(P_0P_\mathrm{F}+P_1P_\mathrm{M}\right)$ is equal to zero at $\rho_m=\rho_m^\star$ for all m. The derivative $\frac{\partial}{\partial\rho_m}\left(P_0P_\mathrm{F}+P_1P_\mathrm{M}\right)$ is equal to

$$\left(\frac{1}{\sigma_0^2}\right)P_0\varphi\left(\frac{\gamma-\mu_0}{\sigma_0}\right)(\gamma-\mu_0)\frac{\partial\sigma_0}{\partial\rho_m}-\left(\frac{1}{\sigma_1^2}\right)P_1\varphi\left(\frac{\gamma-\mu_1}{\sigma_1}\right)(\gamma-\mu_1)\frac{\partial\sigma_1}{\partial\rho_m}, \tag{41}$$

where $\varphi(x)=\frac{1}{\sqrt{2\pi}}e^{-\frac{x^2}{2}}$ and

$$\begin{aligned}\frac{\partial\sigma_i}{\partial\rho_m}=&\frac{\left[\log\left(\frac{q_{m|1}}{q_{M+1|1}}\right)-\log\left(\frac{q_{m|0}}{q_{M+1|0}}\right)\right]^2}{2K(K-\rho_m)\left[\log\left(1-\frac{\rho_m}{K}\right)\right]^3}\times\frac{1}{\sigma_i(1-\bar{p}_{\mathrm{C},m|i})^2}\\&\times\left\{2\bar{p}_{\mathrm{C},m|i}(1-\bar{p}_{\mathrm{C},m|i})-(1-\bar{n}_{m|i})\bar{p}_{\mathrm{S},m|i}\left[\log\left(1-\frac{\rho_m}{K}\right)\right]\right\}.\end{aligned} \tag{42}$$

By substituting (42) into (41) and after some mathematical arrangement, we can show that

$$\begin{aligned}\frac{\partial}{\partial\rho_m}\left(P_0P_\mathrm{F}+P_1P_\mathrm{M}\right)=&\frac{\left[\log\left(\frac{1-q_{m|0}}{q_{m|0}}\right)-\log\left(\frac{1-q_{m|1}}{q_{m|1}}\right)\right]^2}{2K(K-\rho_m)\left[\log\left(1-\frac{\rho_m}{K}\right)\right]^3}\left\{\left[\frac{P_0\varphi\left(\frac{\gamma-\mu_0}{\sigma_0}\right)(\gamma-\mu_0)}{\sigma_0^3(1-\bar{p}_{\mathrm{C},m|0})^2}\right]\right.\\&\times\left[2\bar{p}_{\mathrm{C},m|0}(1-\bar{p}_{\mathrm{C},m|0})-(1-\bar{n}_{m|0})\bar{p}_{\mathrm{S},m|0}\left[\log\left(1-\frac{\rho_m}{K}\right)\right]\right]\\&-\left[\frac{P_1\varphi\left(\frac{\gamma-\mu_1}{\sigma_1}\right)(\gamma-\mu_1)}{\sigma_1^3(1-\bar{p}_{\mathrm{C},m|1})^2}\right]\left[2\bar{p}_{\mathrm{C},m|1}(1-\bar{p}_{\mathrm{C},m|1})\right.\\&\left.\left.-(1-\bar{n}_{m|1})\bar{p}_{\mathrm{S},m|1}\left[\log\left(1-\frac{\rho_m}{K}\right)\right]\right]\right\}.\end{aligned} \tag{43}$$

By setting (43) equal to zero, the term inside the curly brackets must be equal to zero and, after some mathematical arrangement, we have the following equality:

$$\frac{\frac{(1-\bar{p}_{\mathrm{C},m|0})^2}{2\bar{p}_{\mathrm{C},m|0}(1-\bar{p}_{\mathrm{C},m|0})-(1-\bar{n}_{m|0})\bar{p}_{\mathrm{S},m|0}\left[\log\left(1-\frac{\rho_m}{K}\right)\right]}}{\frac{(1-\bar{p}_{\mathrm{C},m|1})^2}{2\bar{p}_{\mathrm{C},m|1}(1-\bar{p}_{\mathrm{C},m|1})-(1-\bar{n}_{m|1})\bar{p}_{\mathrm{S},m|1}\left[\log\left(1-\frac{\rho_m}{K}\right)\right]}}=\left(\frac{\sigma_1}{\sigma_0}\right)^3\left[\frac{P_0\varphi\left(\frac{\gamma-\mu_0}{\sigma_0}\right)(\gamma-\mu_0)}{P_1\varphi\left(\frac{\gamma-\mu_1}{\sigma_1}\right)(\gamma-\mu_1)}\right]. \tag{44}$$

We define the term on the left-hand side of (44) as $g_m(\rho_m)$. Since the term on the right-hand side of (44) is a constant (given $\rho_1^\star$, $\rho_2^\star$, ..., $\rho_M^\star$), we obtain (21). In addition, with properly choosing γ, where $\mu_0\le\gamma\le\mu_1$, we will have $\gamma-\mu_0\ge0$ and $\gamma-\mu_1\le0$. As a result, (22) is less than or equal to zero. In addition, we will have $g_m(\rho_m^\star)\le0$ for all m.

Appendix E: Proof of Proposition 5

First, we will prove (26). Clearly, when $\mu_0 \leq \gamma \leq \mu_1$, from (17) and (18), the transmission probabilities maximizing P_{D} (or minimizing P_{F}, respectively) are the transmission probabilities minimizing σ_1^2 (or minimizing σ_0^2, respectively). Let $\boldsymbol{\rho}_{\mathbf{1}}^{\star}$ and $\boldsymbol{\rho}_{\mathbf{0}}^{\star}$ be the transmission probabilities maximizing P_{D} and minimizing P_{F}, respectively, where $\boldsymbol{\rho}_{\boldsymbol{i}}^{\star} = (\rho_{1|i}^{\star}, \rho_{2|i}^{\star}, \ldots, \rho_{M|i}^{\star})$ and $\rho_{m|i}^{\star}$ is the transmission probability at the mth frame. Therefore, finding the transmission probabilities $\boldsymbol{\rho}_{\boldsymbol{i}}^{\star}$ can be written as the following optimization problem:

$$\boldsymbol{\rho}_{\boldsymbol{i}}^{\star} = \underset{\boldsymbol{\rho}\in[0,1]^M}{\arg\min}\ \sigma_i^2. \tag{45}$$

Considering the variance σ_i^2 defined in (16) shows that the variance σ_i^2 is a summation of M terms, where each term is individually a function of ρ_m. Therefore, the optimization problem above is separable (to M individual optimization problems). As a result, we can find the transmission probability $\rho_{m|i}^{\star}$ from the following optimization problem:

$$\rho_{m|i}^{\star} = \underset{\rho_m\in[0,1]}{\arg\max} \left(\frac{1-\bar{p}_{\mathrm{C},m|i}}{\bar{p}_{\mathrm{C},m|i}}\right)\left[\log\left(1-\frac{\rho_m}{K}\right)\right]^2. \tag{46}$$

Note that the objective function in (46) is inversely proportional to the variance υ_m^2 in (11). Therefore, the optimization problem (46) indicates that the transmission probability $\rho_{m|i}^{\star}$ is the transmission probability minimizing the population estimate's variance υ_m^2.

The necessary condition for the optimal transmission probabilities $\rho_{m|i}^{\star}$ in (46) is that the function $\frac{\partial}{\partial\rho_m}\left(\frac{1-\bar{p}_{\mathrm{C},m|i}}{\bar{p}_{\mathrm{C},m|i}}\right)\left[\log(1-\frac{\rho_m}{K})\right]^2$ is equal to zero at $\rho_m = \rho_m^{\star}$ for all m. The derivative $\frac{\partial}{\partial\rho_m}\left(\frac{1-\bar{p}_{\mathrm{C},m|i}}{\bar{p}_{\mathrm{C},m|i}}\right)\left[\log(1-\frac{\rho_m}{K})\right]^2$ is equal to

$$\left\{\frac{(1-\bar{n}_{m|i})\bar{p}_{\mathrm{S},m|i}\left[\log\left(1-\frac{\rho_m}{K}\right)\right]}{\bar{p}_{\mathrm{C},m|i}} - 2(1-\bar{p}_{\mathrm{C},m|i})\right\}\left[\frac{\log\left(1-\frac{\rho_m}{K}\right)}{\bar{p}_{\mathrm{C},m|i}(K-\rho_m)}\right]. \tag{47}$$

Equivalently, $\rho_{m|i}^{\star}$ is equal to ρ_m that will make the term in the curly brackets equal to zero. Therefore, we have the necessary condition for $\rho_{m|i}^{\star}$ as shown in (26).

Now, we can show that $\rho_m^{\star}$ is between $\rho_{m|0}^{\star}$ and $\rho_{m|1}^{\star}$ as follows. Consider the function $g_m(\rho_m)$ in (20). The function $g_m(\rho_m)$ will approach to $-\infty$ at the ρ_m making the term $2\bar{p}_{\mathrm{C},m|0}(1-\bar{p}_{\mathrm{C},m|0}) - (1-\bar{n}_{m|0})\bar{p}_{\mathrm{S},m|0}\left[\log\left(1-\frac{\rho_m}{K}\right)\right]$ equal to zero. We further notice that this ρ_m is the transmission probability $\rho_{m|0}^{\star}$ minimizing the probability of false alarm from (26). On the other hand, the function $g_m(\rho_m)$ will be zero at the ρ_m making the term $2\bar{p}_{\mathrm{C},m|1}(1-\bar{p}_{\mathrm{C},m|1}) - (1-\bar{n}_{m|1})\bar{p}_{\mathrm{S},m|1}\left[\log\left(1-\frac{\rho_m}{K}\right)\right]$ equal to zero. This ρ_m is the transmission probability $\rho_{m|1}^{\star}$ maximizing the probability of detection. From the necessary condition (iii) in Proposition 4 that $g_m(\rho_m^{\star}) \leq 0$, then, $\rho_m^{\star}$ is between $\rho_{m|0}^{\star}$ and $\rho_{m|1}^{\star}$.

Abbreviations

FC: Fusion center; FDMA: Frequency division multiple access; IID: Independent and identically distributed; MAC: Medium access control; ML: Maximum likelihood; PAC: Parallel access channel; PDF: Probability density function; PMF: Probability mass function; PSRA: Population-splitting-based random access; SNR: Signal-to-noise- ratio; TBMA: Type-based multiple access; TBRA: Type-based random access; TDMA: Time division multiple access; WSN: Wireless sensor network.

Acknowledgements
The author would like to thank the associate editor and the anonymous reviewers for comments and suggestions that contributed to improve the quality of this paper.

Funding
No funding was received for this research work.

Availability of data and materials
Not applicable.

Competing interests
The author declares that he has no competing interests.

Received: 13 September 2019 Accepted: 29 December 2020
Published online: 29 March 2021

References

1. Z. Chair, P.K. Varshney, Optimal data fusion in multiple sensor detection systems. IEEE Trans. Aerosp. Electron. Syst. **AES–22**, 98–101 (1986)
2. R. Viswanathan, P.K. Varshney, Distributed detection with multiple sensors: part I-fundamentals. Proc. IEEE. **85**(1), 54–63 (1997)
3. S.M. Kay, *Fundamentals of Statistical Signal Processing: Detection Theory* (Prentice Hall, Upper Saddle River, NJ)
4. S. Yiu, R. Schober, Nonorthogonal transmission and noncoherent fusion of censored decisions. IEEE Trans. Veh. Technol. **58**(1), 263–273 (2009)
5. A. Lei, R. Schober, Multiple-symbol differential decision fusion for mobile wireless sensor networks. IEEE Trans. Wirel. Commun. **9**(2), 778–790 (2010)
6. F. Li, J.S. Evans, S. Dey, Decision fusion over noncoherent fading multiaccess channels. IEEE Trans. Signal Process. **59**(9), 4367–4380 (2011)
7. T.Y. Chang, T.C. Hsu, Y.W.P. Hong, Exploiting data-dependent transmission control and MAC timing information for distributed detection in sensor networks. IEEE Trans. Signal Process. **58**(3), 1369–1382 (2010)
8. D. Xu, Y. Yao, Contention-based transmission for decentralized detection. IEEE Trans. Wirel. Commun. **11**(4), 1334–1342 (2012)
9. S. Laitrakun, E.J. Coyle, Reliability-based splitting algorithms for time-constrained distributed detection in random-access channels. IEEE Trans. Signal Process. **62**(21), 5536–5551 (2014)
10. D. Ciuonzo, G. Romano, P.S. Rossi, Channel-aware decision fusion in distributed MIMO wireless sensor networks: decode-and-fuse vs. decode-then-fuse. IEEE Trans. Wirel. Commun. **11**(8), 2976–2985 (2012)
11. I. Nevat, G.W. Peters, I.B. Collings, Distributed detection in sensor networks over fading channels with multiple antennas at the fusion centre. IEEE Trans. Signal Process. **62**(3), 671–683 (2014)
12. D. Ciuonzo, P. Salvo Rossi, S. Dey, Massive MIMO channel-aware decision fusion. IEEE Trans. Signal Process. **63**(3), 604–619 (2015)
13. P. Salvo Rossi, D. Ciuonzo, K. Kansanen, T. Ekman, Performance analysis of energy detection for MIMO decision fusion in wireless sensor networks over arbitrary fading channels. IEEE Trans. Wirel. Commun. **15**(11), 7794–7806 (2016)
14. B. Chen, R. Jiang, T. Kasetkasem, P.K. Varshney, Channel aware decision fusion in wireless sensor networks. IEEE Trans. Signal Process. **52**(12), 3454–3458 (2004)
15. R. Jiang, B. Chen, Fusion of censored decisions in wireless sensor networks. IEEE Trans. Wirel. Commun. **4**(6), 2668–2673 (2005)
16. R. Niu, B. Chen, P.K. Varshney, Fusion of decisions transmitted over Rayleigh fading channels in wireless sensor networks. IEEE Trans. Signal Process. **54**(3), 1018–1027 (2006)
17. K. Eritmen, M. Keskinoz, Distributed decision fusion over fading channels in hierarchical wireless sensor networks. Wirel. Netw. **20**(5), 987–1002 (2014)
18. S.A. Aldalahmeh, M. Ghogho, D. McLernon, E. Nurellari, Optimal fusion rule for distributed detection in clustered wireless sensor networks. EURASIP J. Adv. Signal Process. **2016**(1), 5 (2016)
19. J. Luo, Z. Liu, Serial distributed detection for wireless sensor networks with sensor failure. EURASIP J. Wirel. Commun. Netw. **2017**(1), 123 (2017)
20. S. Marano, V. Matta, P. Willett, L. Tong, Cross-layer design of sequential detectors in sensor networks. IEEE Trans. Signal Process. **54**(11), 4105–4117 (2006)
21. A. Tantawy, X. Koutsoukos, G. Biswas, Cross-layer design for decentralized detection in WSNs. EURASIP J. Adv. Signal Process. **2014**(1), 43 (2014)
22. C. Rago, P. Willett, Y. Bar-Shalom, Censoring sensors: a low-communication-rate scheme for distributed detection. IEEE Trans. Aerosp. Electron. Syst. **32**(2), 554–568 (1996)
23. V.W. Cheng, T.Y. Wang, Performance analysis of distributed decision fusion using a multilevel censoring scheme in wireless sensor networks. IEEE Trans. Veh. Technol. **61**(4), 1610–1619 (2012)
24. R.S. Blum, B.M. Sadler, Energy efficient signal detection in sensor networks using ordered transmissions. IEEE Trans. Signal Process. **56**(7), 3229–3235 (2008)
25. L. Hesham, A. Sultan, M. Nafie, F. Digham, Distributed spectrum sensing with sequential ordered transmissions to a cognitive fusion center. IEEE Trans. Signal Process. **60**(5), 2524–2538 (2012)
26. Y. Yao, Group-ordered SPRT for decentralized detection. IEEE Trans. Inf. Theory **58**(6), 3564–3574 (2012)

27. G.T. Whipps, E. Ertin, R.L. Moses, Distributed detection of binary with collisions in a large, random network. IEEE Trans. Signal Process. **63**(6), 1477–1489 (2015)
28. S. Laitrakun, E.J. Coyle, Collision-aware sequential distributed detection with sensor censoring in random-access WSNs, in *Proceedings of the 12th International Conference on Electrical Engineering/Electronics, Computer, Telecommunications and Information Technology (ECTI-CON)*. (Thailand, 2015), pp. 1–6
29. S. Laitrakun, E.J. Coyle, Collision-aware composite hypothesis testing in random-access WSNs with sensor censoring, in *Proceedings of the International Computer Science and Engineering Conference (ICSEC)*. (Thailand, 2015), pp. 1–6
30. S. Laitrakun, Rao-test fusion rules of uncensored decisions transmitted over a collision channel, in *Proceedings of the 21st International Symposium on Wireless Personal Multimedia Communications (WPMC)*. (Thailand, 2018), pp. 495–500
31. D. Bertsekas, R. Gallager, *Data Networks*, 2nd edn. (Prentice Hall, Upper Saddle River, 1992)
32. L. Yang, H. Zhu, H. Wang, K. Kang, H. Qian, Data censoring with network lifetime constraint in wireless sensor networks. Digit Signal Process. **92**, 73–81 (2019)
33. G. Mergen, V. Naware, L. Tong, Asymptotic detection performance of type-based multiple access over multiaccess fading channels. IEEE Trans. Signal Process. **55**(3), 1081–1092 (2007)
34. K. Liu, A.M. Sayeed, Type-based decentralized detection in wireless sensor networks. IEEE Trans. Signal Process. **55**(5), 1899–1910 (2007)
35. A. Anandkumar, L. Tong, Type-based random access for distributed detection over multiaccess fading channels. IEEE Trans. Signal Process. **55**(10), 5032–5043 (2007)
36. S. Laitrakun, E.J. Coyle, Collision-aware distributed estimation in WSNs using sensor-censoring random access, in *Proceedings of the Military Communications Conference (MILCOM)*. (USA, 2015), pp. 1039–1045
37. S. Laitrakun, D. Phanish, E.J. Coyle, Energy-efficient clustering and collision-aware distributed detection/estimation in random-access-based WSNs, in *Data Fusion in Wireless Sensor Networks: A Statistical Signal Processing Perspective*, ed. by D. Ciuonzo, P.S. Rossi (The Institution of Engineering and Technology, London, 2019), pp. 81–110
38. S.A. Kassam, Optimum quantization for signal detection. IEEE Trans. Commun. **COM–25**(5), 479–484 (1997)
39. R. Niu, P.K. Varshney, Target location estimation in sensor networks with quantized data. IEEE Trans. Signal Process. **54**(12), 4519–4528 (2006)
40. J. Fang, H. Li, Distributed adaptive quantization for wireless sensor networks: from delta modulation to maximum likelihood. IEEE Trans. Signal Process. **56**(10), 5246–5257 (2008)
41. V. Kapnadak, M. Senel, E.J. Coyle, Distributed iterative quantization for interference characterization in wireless networks. Digit. Signal Process. **22**(1), 96–105 (2012)
42. F. Gao, F.G. Lili, H. Li, J. Liu, J. Fang, Quantizer design for distributed GLRT detection of weak signals in wireless sensor networks. IEEE Trans. Wirel. Commun. **14**(4), 2032–2042 (2015)
43. S. Laitrakun, E.J. Coyle, Optimizing the collection of local decisions for time-constrained distributed detection in WSNs, in *Proceedings of the IEEE International Conference on Computer Communications (INFOCOM)*. (Italy, 2013), pp. 1923–1931

Publisher's Note